

Lawrence Berkeley National Laboratory

LBL Publications

Title

Combined Experimental and Computational Study on the Unimolecular Decomposition of JP-8 Jet Fuel Surrogates. II: n-Dodecane (n-C₁₂H₂₆)

Permalink

<https://escholarship.org/uc/item/7nb181bp>

Journal

The Journal of Physical Chemistry A, 121(6)

ISSN

1089-5639

Authors

Zhao, Long

Yang, Tao

Kaiser, Ralf I

et al.

Publication Date

2017-02-16

DOI

10.1021/acs.jpca.6b11817

Peer reviewed

**A Combined Experimental and Computational Study on the Unimolecular
Decomposition of JP-8 Jet Fuel Surrogates II: *n*-Dodecane (*n*-C₁₂H₂₆)**

Long Zhao, Tao Yang, Ralf I. Kaiser*

Department of Chemistry, University of Hawaii at Manoa, Honolulu, Hawaii, 96822

Tyler P. Troy, Musahid Ahmed*

*Chemical Sciences Division, Lawrence Berkeley National Laboratory, Berkeley, California
94720*

Joao Marcelo Ribeiro, Daniel Belisario-Lara, Alexander M. Mebel*

*Department of Chemistry and Biochemistry, Florida International University, Miami, Florida
33199*

ABSTRACT

We investigated temperature-dependent products in the pyrolysis of helium-seeded *n*-dodecane, which represents a surrogate of the *n*-alkane fraction of Jet Propellant-8 (JP-8) aviation fuel. The experiments were performed in a high temperature chemical reactor over a temperature range of 1,200 K to 1,600 K at a pressure of 600 Torr, with *in situ* identification of the nascent products in a supersonic molecular beam using single photon vacuum ultraviolet (VUV) photoionization coupled with the analysis of the ions in a reflectron time-of-flight mass spectrometer (ReTOF). For the first time, the initial decomposition products of *n*-dodecane - including radicals and thermally labile closed-shell species were probed in experiments, which effectively exclude mass growth processes. Fifteen different products were identified, such as molecular hydrogen (H_2), C2 to C7 1-alkenes [ethylene (C_2H_4) to 1-heptene (C_7H_{14})], C1-C3 radicals [methyl (CH_3), ethyl (C_2H_5), allyl (C_3H_5)], small C1-C3 hydrocarbons [acetylene (C_2H_2), allene (C_3H_4), methylacetylene C_3H_4], as well as the reaction products [1,3-butadiene (C_4H_6), 2-butene (C_4H_8)] attributed to higher-order processes. Electronic structure calculations carried out at the G3(CCSD,MP2)//B3LYP/6-311G(d,p) level of theory combined with RRKM/Master Equation of rate constants for relevant reaction steps showed that *n*-dodecane decomposes initially by a non-terminal C-C bond cleavage and producing a mixture of alkyl radicals from ethyl to decyl with approximately equal branching ratios. The alkyl radicals appear to be unstable under the experimental conditions and to rapidly dissociate either directly by C-C bond β -scission to produce ethylene (C_2H_4) plus a smaller 1-alkyl radical with the number of carbon atoms diminished by two or via 1,5-, 1,6-, or 1,7- 1,4-, 1,9-, or 1,8-H shifts followed by C-C β -scission producing alkenes from propene to 1-nonene together with smaller 1-alkyl radicals. The stability and hence the branching ratios of higher alkenes decrease as temperature increases. The C-C β -scission continues all the way to the propyl radical (C_3H_7), which dissociates to methyl (CH_3) plus ethylene (C_2H_4). In addition, at higher temperatures, another mechanism can contribute, in which hydrogen atoms abstract hydrogen from $C_{12}H_{26}$ producing various *n*-dodecyl radicals and these radicals then decompose by C-C bond β -scission to C3 to C11 alkenes.

1. INTRODUCTION

Jet Propellant-8 (JP-8) represents a kerosene-based jet fuel which is widely used by the US military. It is comprised of hundreds of hydrocarbons which include aliphatic molecules (33-61% *n*-alkanes and isoalkanes; 1-5% olefins), monocyclic ‘paraffins’ (10-20%), alkyl-substituted benzenes (12-22%), and polycyclic aromatic hydrocarbons (PAHs) (10-20%). Combustion scientists have been exploiting surrogate fuels in an attempt to convincingly model the performance along with emission characteristics of JP-8 engines.¹⁻²⁴ While single-component surrogate fuels are suitable to replicate combustion efficiencies, multi-component surrogates are essential to adequately model the chemistry of soot formation and flames.²⁵

These kinetic models require precise input parameters and an accurate knowledge of the initial steps, which initiate bond rupture in JP-8 surrogates. These processes essentially supply a pool of highly reactive radicals - often aromatic radicals (AR) and resonantly stabilized free radicals (RSFRs) - ultimately managing the autoignition and successive oxidation processes under combustion relevant conditions of up to 1,600 K and pressures up to a few atmospheres.^{10,26-29} Previous experimental studies on the decomposition of the aliphatic component of JP-8 exploited *n*-dodecane (C₁₂H₂₆) as surrogates. These studies utilized high pressure shock tubes, flow reactors, jet stirred reactors, and micro reactors covering temperatures from 673 K to 1739 K and pressures from 0.68 atm to 100 atm with diverging residence times of up to a few thousands of milliseconds (Table 1). In principle, these experiments revealed that the decomposition and ‘pyrolysis’ of these surrogates lead to smaller C1 to C12 hydrocarbon molecules, but also reveal mass growth processed leading eventually to polycyclic aromatic hydrocarbons (PAHs) (Table S1).

The studies of *n*-dodecane thermal decomposition can be traced back to the 1980s. With high-pressure single pulse shock tube setups, Malewicki and Brezinsky³⁰ performed an experimental and modeling study on the pyrolysis and oxidation of *n*-dodecane. The experiment covered the temperature range from 867 to 1739 K, pressures from 19 to 74 atm, reaction times from 1.15 to 3.47 ms, and equivalence ratios from 0.46 to 2.05, and ∞. They measured the major hydrocarbon intermediates during *n*-dodecane pyrolysis experiments including ethylene (C₂H₄), methane (CH₄), propylene (C₃H₆), acetylene (C₂H₂), ethane (C₂H₆), 1-butene (C₄H₈), 1,3-butadiene (C₄H₆), 1-hexene (C₆H₁₂), 1-pentene (C₅H₁₀), 1-heptene (C₇H₁₄), 1-octene (C₈H₁₆), vinylacetylene (C₄H₄), 1-nonene (C₉H₁₈), and 1-decene (C₁₀H₂₀). Davidson et al.³¹ utilized high-

pressure shock tubes to detect the pyrolysis of three hydrocarbons including *n*-dodecane, methylcyclohexane, and *iso*-cetane from 990 to 1520 K at 17 to 23 atm. The fuel decomposition rates and ethylene yields were reported. They found that *iso*-cetane decomposes much faster than *n*-dodecane and MCH decomposes much slower than *n*-dodecane. *n*-dodecane decomposition resulted in negligible amounts of propene and 1-butene at the conditions of 20 atm and 1000-1500 K. Later, Banerjee et al.³² performed an experimental and modeling study on the pyrolysis and oxidation of *n*-dodecane exploiting a flow reactor and a temperature range of 1,000 K to 1,300 K, a pressure of 1 atm, and a residence time up to 40 ms. They found that over the temperature of 1,000 K, the process can be divided into two stages, decomposition of the fuel and its intermediates. The second step of intermediate decomposition is always rate limiting. Bounaceur et al.³³ presented experimental results for *n*-dodecane pyrolysis from 950 to 1,050 K at 1 atm. The time-history of several hydrocarbon intermediates and final products were measured including methane (CH₄), ethane (C₂H₆), acetylene (C₂H₂), ethylene (C₂H₄), propene (C₃H₆), 1-butene (C₄H₈), 1,3-butadiene (C₄H₆), 1-pentene (C₅H₁₀), 1-hexene (C₆H₁₂), 1,3-hexadiene (C₆H₁₀) and 1-heptene (C₇H₁₄). By using a jet-stirred reactor, Herbinet et al.³⁴ carried out an experimental and kinetic modeling study on the thermal decomposition of *n*-dodecane in the temperature range from 773 to 1,073 K at residence times between 1 and 5 s at atmospheric pressure. This study observed products including hydrogen (H₂), methane (CH₄), ethane (C₂H₆), 1,3-butadiene (C₄H₆), and 1-alkenes from ethylene (C₂H₄) to 1-undecene (C₁₁H₂₂). And at higher temperatures and residence times, mass growth processes to monocyclic and polycyclic aromatic species were observed. Zhou et al.³⁵ presented a flow reactor pyrolysis study on several higher molecular weight straight-chain alkanes including *n*-dodecane within a temperature range from 623 K to 893 K at atmospheric pressure. The residence time ranged from 3.3 to 12.3 s. In this study, the authors found the 1-alkene selectivity strongly depends upon the system pressure in the pyrolysis of straight-chain alkanes as major products. The lower the pressure, the higher this selectivity. Yu and Eser³⁶⁻³⁷ used a stainless steel tubing bomb reactor to study the near-critical and supercritical phase thermal decomposition of C10-C14 alkanes at 673K to 723 K and 1-10 MPa. They observed the relative yields of the primary (*n*-alkanes and 1-alkenes) and secondary products (*cis*- and *trans*-2-alkenes, smaller normal and branched alkanes) are dependent upon the reaction conditions (pressure/loading ratio, conversion, and temperature). As pressure increases,

the yields of C6-Cm-1 *n*-alkanes and Cm+ alkanes increase and the yields of 1-alkenes and C1-C3 *n*-alkanes decrease. And high temperature favors the formation of 1-alkenes.

Besides the aforementioned experimental studies, kinetic modeling projects on *n*-dodecane pyrolysis were also carried in the recent years. With MAMOX++ program, Ranzi et al.³⁸ generated a wide-range kinetic modeling study of the pyrolysis, partial oxidation and combustion of large *n*-alkanes, including *n*-decane, *n*-dodecane and *n*-hexadecane. Later, they assembled the mechanisms for *n*-heptane and *n*-dodecane oxidation and reduced them, with the lumping approach proposed for the detailed mechanism³⁹. Battin-Leclerc et al.^{34,40} built up kinetic mechanisms of *n*-dodecane with EXGAS software to simulate several experimental data including JSR pyrolysis, JSR oxidation, shock tube ignition delay times, turbulent flow reactor oxidation, for both high and low temperatures. In their studies, the NTC (negative temperature coefficient) region was reproduced for the JSR and shock tube experiments. Wang et al.⁴¹ proposed a detailed kinetic model consisted of 1306 reactions and 171 species for the combustion of *n*-alkanes up to *n*-dodecane above 850 K, validated against several experimental data including flow reactor pyrolysis, JSR pyrolysis, laminar flame speeds and shock tube ignition delay times. In addition to their experimental study, Malewicki and Brezinsky³⁰ also performed a modeling study on the pyrolysis and oxidation of *n*-decane and *n*-dodecane. Based on their present and some previous literature data, they revised the kinetic model by Dooley et al.⁴² Of particular interest, Westbrook and coworkers⁴³ carried out a comprehensive detailed chemical kinetic mechanism for *n*-alkanes from *n*-octane to *n*-hexadecane. Their mechanism was designed to reproduce *n*-alkane oxidation in both low and high temperatures, and validated through extensive comparisons between computed and experimental data from a wide variety of different sources, including flow reactor pyrolysis, JSR pyrolysis, JSR oxidation, shock tube and RCM ignition delay times. Recently, Narayanaswamy et al.⁴⁴ also presented a comprehensive kinetic modeling study for oxidation and pyrolysis of *n*-dodecane. They simulated several experimental data including ignition delay times, shock tube oxidation/pyrolysis speciation, flow reactor oxidation and burning velocity. The proposed reaction mechanism can describe the kinetics of *n*-dodecane, as well as that of *n*-heptane, *iso*-octane, and some substituted aromatics (toluene, styrene, ethylbenzene, *m*-xylene and 1-methylnaphthalene), which are important components of transportation fuel surrogates.

Very recently, we started a systematic research program to untangle the decomposition mechanisms of JP-8 surrogates by pyrolyzing helium-seeded *n*-decane ($n\text{-C}_{10}\text{H}_{22}$) in a chemical reactor at pressures of 600 Torr over a temperature range from 1,100 K to 1,600 K⁴⁵. The product distribution - including radicals and thermally labile closed shell species - was probed on line and *in situ* in a supersonic molecular beam utilizing soft photoionization with single photon vacuum ultraviolet (VUV) photons followed by a mass spectroscopic analysis of the ions in a reflectron time-of-flight mass spectrometer (Re-TOF), which can be utilized to identify and quantify products in the pyrolysis, especially radicals and isomers.⁴⁶⁻⁵⁷ By limiting the residence time in the reactor to a couple of tens of microseconds, our major objectives are to explore the *initial reaction products* and aim to eliminate successive reactions of the initially formed species, which can lead to molecular mass growth processes. These studies reported multiple lower-mass C3 to C7 hydrocarbons including alkenes, alkynes and dienes along with C1 (methane) and C2 (acetylene, ethylene) as final products. Also, five radicals were observed in the *n*-decane pyrolysis including methyl, vinyl, ethyl, propargyl, and allyl. Further, the study presented branching ratios along with the underlying decomposition mechanisms. Here, we expand our studies to investigate via a combined theoretical and experimental strategy, the decomposition mechanisms of *n*-dodecane ($\text{C}_{12}\text{H}_{26}$) within the pyrolytic reactor and compare our findings with those data from previous high pressure shock tubes, flow reactors, and jet stirred reactor studies. It is our goal to provide both qualitative and quantitative identification of all nascent decomposition products (radicals and closed shell molecules along with their structural isomers), the fundamental decomposition mechanisms, and reveal how their branching ratios depend on the temperature of the reactor. These data are of critical importance to the JP-8 modeling community to eventually optimize combustion efficiency and limit the production of toxic byproducts such as carcinogenic and mutagenic PAHs.

2. EXPERIMENTAL APPROACH

The experiments were conducted at the Advanced Light Source (ALS) at the Chemical Dynamics Beamline (9.0.2.) exploiting a ‘pyrolytic reactor’. The experiment apparatus has been described before.⁵⁸⁻⁶⁸ Briefly, the high temperature chemical reactor consists of a resistively heated silicon carbide (SiC) tube of 20 mm in length and 1 mm inner diameter. A gas mixture at a pressure of 600 Torr containing 0.0027% *n*-dodecane ($\text{C}_{12}\text{H}_{26}$) (Sigma-Aldrich; 99%+) in helium carrier gas (He; Airgas; 99.999%) is prepared by bubbling helium gas through *n*-

dodecane stored in a stainless-steel bubbler held at 271 ± 1 K, the vapor pressure being 0.016 Torr at this temperature. The gas mixture was introduced into a resistively heated silicon carbide tube held at temperatures ranging from 1200 K to $1,600 \pm 5$ K as monitored by a Type-C thermocouple in steps of 100 K. Here, photoionization efficiency (PIE) scans were performed with 0.05 eV intervals from 8.00 eV to 11.50 eV. For each temperature, the PIE scans were recorded three times and averaged; the experimental uncertainties were derived within one sigma as shown in the shaded areas in Fig. 2. A set of additional mass spectra was also taken at 15.5 eV to get extra information on hydrogen and methane (if they exist), which cannot be ionized at 11.5 eV. Pressures in the reactor at axial distances of 10 mm and 15 mm from the inlet are predicted to drop to about 60% and 30% of the inlet pressure based on simulations.⁶⁹ This would result in typically three to four (1,600 K) collisions of a dodecane molecule with the helium atoms at these distances.

PIE analysis^{46-47,55,57} and branching ratios were also performed to reveal the tendency of the products along with the temperature increasing. The detailed methods for PIE analysis branching ratio calculation were also introduced in our previous work⁴⁵. In brief, the PIE curves were fitted based on the known photoionization cross sections of corresponding species from the online database⁷⁰. For the branching ratio calculation, for a certain species, since the ion count (normalized by the photon fluxes) presents a direct proportional relationship with the mole fraction (concentration), photoionization cross section and mass discrimination ($S_i(T, E) \propto X_i(T) \cdot \sigma_i(E) \cdot D_i$),⁵⁵ and the ion counts were measured in the experiment, the cross sections can be looked up in the database, then the relationship between the concentrations of individual

products can be calculated ($\frac{X_i(T)}{X_j(T)} = \frac{S_i(T, E)}{S_j(T, E)} \cdot \frac{\sigma_j(E)}{\sigma_i(E)} \cdot \frac{D_j}{D_i}$). Subsequently the branching ratios

can be worked out. Here, the branching ratios were computed by exploiting photoionization known cross sections of 9.5, 10.0, 10.5, 11.0, 11.5, and 15.5 eV with data obtained at 15.5 eV used to calculate the branching ratios of methane and hydrogen. The mass discrimination factors were taken from Reference⁶⁸. The uncertainties of the photoionization cross sections of 15-20% were also taken into consideration.⁵⁶ In this work, the uncertainties of the cross section are chosen as 20%.

3. COMPUTATIONAL METHODS

Geometries of *n*-dodecane, its primary and secondary decomposition products, and transition states for secondary decomposition reactions (C-C bond β -scissions) and for direct H atom abstractions by hydrogen atoms have been optimized using the density functional B3LYP/6-311G(d,p) method. Vibrational frequencies of various stationary structures have been computed at the same level of theory. Then, relative energies for all optimized structures have been reevaluated by single-point calculations at the G3(CCSD,MP2) level of theory⁷¹⁻⁷³ with B3LYP/6-311G(d,p) zero-point vibrational energy corrections (ZPE), including the empirical higher level correction (HLC)⁷³ and using B3LYP/6-311G(d,p) optimized geometries. The inclusion of the HLC increases the calculated strengths of C-H bonds by 7 kJ/mol, decreases relative energies of transition states and products for the $C_{12}H_{26} + H \rightarrow C_{12}H_{25} + H_2$ hydrogen atom abstraction reactions also by 7 kJ/mol, is insignificant for C-C bond cleavages, and zero by definition for C-C bond β -scissions. The G3(CCSD,MP2)//B3LYP theoretical level has been shown to provide ‘chemical accuracy’ within 3-6 kJ/mol in terms of average absolute deviations of relative energies of various stationary structures.⁷² The ab initio calculations were performed using the GAUSSIAN 09⁷⁴ and MOLPRO 2010⁷⁵ program packages.

Rate constants for primary and secondary reactions involved in the pyrolysis of *n*-dodecane have been calculated using the RRKM/Master Equation approach⁷⁶ with the MESS package⁷⁷, generally utilizing the Rigid-Rotor, Harmonic-Oscillator (RRHO) approximation for the evaluation of partition functions for molecular complexes and transition states. Collisional energy transfer rates in the master equation were expressed using the “exponential down” model,⁷⁸ with the temperature dependence of the range parameter α for the deactivating wing of the energy transfer function expressed as $\alpha(T) = \alpha_{300}(T/300 \text{ K})^n$, with $n = 0.86$ and $\alpha_{300} = 228 \text{ cm}^{-1}$ obtained earlier from classical trajectories calculations as ‘universal’ parameters for hydrocarbons in the nitrogen bath gas.⁷⁹ We used the Lennard-Jones parameters (ϵ/cm^{-1} , $\sigma/\text{\AA}$) = (253, 5.16) for the *n*-dodecane/nitrogen system derived by Jasper et al.⁷⁸ based on the fit of results using the “one-dimensional optimization” method⁸⁰.

Since our goal in this work is both qualitative and quantitative evaluation of relative yields of various products at different stages of the pyrolysis in order to account for the observed experimental results, we used a simplified approximation to treat C-C and C-H single bond cleavages in the original *n*-dodecane molecule occurring without barriers. In particular, rate

constants for these reactions were calculated using phase space theory with empirical potential energy parameters selected in such a way that the rate constants for the reverse $C_xH_y + C_{12-x}H_{26-y}$ and $C_{12}H_{25} + H$ radical recombination reactions reproduce the rate constants for the prototype $CH_3 + CH_3$ and $C_2H_5 + H$ reactions in the experimental 1,200-1,600 K temperature interval studied earlier by Klippenstein and co-workers⁸¹⁻⁸² using the most accurate up-to-date theoretical approach, variable reaction coordinated transition state theory (VRC-TST). Another theoretical issue is the appropriate treatment of soft normal modes in $C_{12}H_{26}$ and $C_{12}H_{25}$ radicals, which are represented by convoluted coupled hindered rotations. Identification of such hindered rotors and evaluation of their potential energy profiles in long alkanes is an extremely complex task. However, in our previous work, we showed that in smaller 1-alkyl radicals, from C_3H_7 to C_9H_{19} , the replacement of harmonic oscillators with hindered rotors increased the computed C-C β -scission rate constants by 8-41% at 1000 K and by only 2-25% at 1,600 K.⁴⁵ Here, all calculations have been performed within RRHO keeping in mind the above mentioned error bars in rate constants. The anticipated errors in ratios of rate constants are expected to be smaller than the errors in their absolute values due to cancelations of similar inaccuracies.

4. EXPERIMENTAL RESULTS

Figure 1 exhibits the mass spectra collected during the pyrolysis of *n*-dodecane ($C_{12}H_{26}$, $m/z = 170$) at the energy of 10.0 eV covering the temperature range from 1,200 K to 1,600 K. The photon energy was chosen to be 10.0 eV to avoid the formation of fragment ions from dissociative photoionization of *n*-dodecane at photon energies higher than 10.5 eV. These fragments are labeled as '*n*-dodecane fragment' in Figure 2. The mass spectrometric data alone provide evidence of ion counts from $m/z = 15$ to $m/z = 98$ along with the parent ions of the ionized *n*-dodecane precursor at $m/z = 170$. No ion counts of molecules heavier than *n*-dodecane were observed at the experiment temperature. This requirement represents a crucial prerequisite for the extraction of the *initial* pyrolysis products of *n*-dodecane. The detected mass-to-charge ratios, as well as the chemical formulae and chemical structures of the products, are listed in Tables 2 and 3; species observed for the first time in a pyrolysis experiment of *n*-dodecane are emphasized in bold. The corresponding photoionization efficiency (PIE) curves along with the best fits are visualized in Fig. 2 for all temperatures from 1,200 K to 1,600 K. As outlined in the experimental section, the individual PIE curves from $m/z = 15$ to $m/z = 170$ were fitted with the linear combination of known PIE curves of the corresponding species. Generally, the black lines

in Fig. 2 represent the experimental data of PIE curves in this work with the shaded area exhibiting the experimental uncertainties. The red lines are the overall best fit to the PIE curves. If the PIE curves have contributors of more than one species, the blue, green and purple lines are referred to the individual components. Literature PIE curves are taken from the combustion chemistry database⁷⁰ and are individually referenced as well (Table 4). A detailed analysis of the temperature dependence of the PIE curves (Figure 2) as outlined above reveals interesting trends.

First, the intensity of the parent ion of *n*-dodecane ($m/z = 170$) decreases as the temperature drops from 60% (1,200 K) via 48% (1,300 K), 9% (1,400 K), and eventually vanishes at 1,500 K. This suggests that the decomposition of the *n*-dodecane precursor is complete at 1,500 K.

Second, as compiled in Table 3, as the temperature increases, the number of pyrolysis products first rises from eight C1 to C7 species at 1,200 K to ten (1,300 K), twelve (1,400 K), fifteen products (1,500 K) before ultimately decreasing to twelve C1-C4 products (1,600 K). This trend proposes that as the temperature increases beyond 1,400 K, degradation occurs for the initial higher molecular weight products from C4 to C6 hydrocarbons, especially for C5 and C6 transients, which are completely consumed at 1,600 K.

Third, we have identified 15 products, which can be arranged into six groups. i) a homologues series of alkenes [C2-C7; ethylene (C₂H₄), propene (C₃H₆), 1-butene (C₄H₈), 2-butene (C₄H₈), 1-pentene (C₅H₁₀), 1-hexene (C₆H₁₂) and 1-heptene (C₇H₁₄)], ii) diene [1,3-butadiene (C₄H₆)], iii) cumulene [allene (C₃H₄)], iv) alkynes (acetylene (C₂H₂), methylacetylene (C₃H₄)), v) radicals [methyl (CH₃), ethyl (C₂H₅), allyl (C₃H₅)], and vi) smaller products [hydrogen (H₂)]. The appearance energies (ionization onsets) of these products as determined in our experiments agree very well with the adiabatic ionization energies as compiled in Table 5 with deviations of less than 0.05 eV in cases of excellent signal-to-noise ratios of the PIE curves, but not more than 0.08 eV otherwise. Among these species, it is important to highlight that this technique is ideally suited to detect C1 to C3 radical species as pyrolysis products, among them the methyl (CH₃), ethyl (C₂H₅) and allyl (C₃H₅) radicals being detected for the first time in *n*-dodecane pyrolysis experiments. Compared with our previous *n*-decane investigation, methane, vinyl and propargyl were not observed in this *n*-dodecane pyrolysis. There might be two reasons: 1) the initial concentration of *n*-dodecane is lower by 88% compared with that of *n*-decane due to

the lower vapor pressure;⁴⁵ 2) the branching ratios of these three species is much lower with respect to the other products.

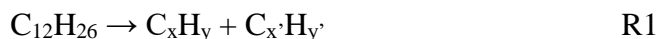
Fourth, Table 3 and Fig. 3 quantify that ethylene (C_2H_4) represents the major decomposition products of *n*-dodecane over the complete temperature range increasing from about 30% to 60% from 1,200 K to 1,600 K. It is important to highlight that simultaneously the branching ratios of the chemically related ethyl radical (C_2H_5) decrease from about 20% at 1,200 K to less than 1% at 1,500 K. Acetylene (C_2H_2) represents only minor products of less than 2% at most (1,600 K). The initial appearance temperature of acetylene was found to be 1,500 K; its branching ratio increases with rising temperature suggesting that acetylene represents one of the final, thermally stable products generated from higher molecular weight intermediates. Besides these C2 products, propene (C_3H_6) with branching ratios slightly decreasing from about 13% (1,200 K) to 8% (1,600 K) represents the most prominent C3 product. The C3 close shells products allene and methylacetylene (C_3H_4) only contribute a total from about 0.6% (1,400 K) to 6.7% (1,600 K) to the total branching. The C3 radical allyl (C_3H_5) appears at 1,300 K. The branching ratio increases from 4% at 1,300 K to 9% at 1,500 K, and abruptly drops to 2% at 1,600 K, suggesting that allyl represents a dynamic intermediate that is simultaneously decomposing while being produced. The branching ratios of the C4 to C7 alkenes steadily decrease as the temperature rises from 1,200 K to 1,600 K indicating that these alkenes decompose in consecutive processes. Therefore, this trend proposes that the C4 to C7 hydrocarbons can be classified as reaction intermediates. As a matter of fact, at 1,600 K, 1-pentene, 1-hexene, and 1-heptene are completely decomposed and hence undetectable. At 1,600 K, among the C4 to C7 products, only 1,3-butadiene (C_4H_6), 1-butene and 2-butene survive at fractions of less than 1%. Finally, it should be noted that our studies also detected molecular hydrogen (H_2) along with the methyl radical (CH_3). Both of them increase with temperature up to 1,500 K, where methyl drops off at 1,600 K (the branching ratio of methyl drops from 13% to 9%), while molecular hydrogen keeps increasing.

Finally, the branching ratios as compiled in Table 3 allow us to determine the overall mass balance of the experiments. The overall carbon-to-hydrogen (C/H) ratio is plotted in Figure 4 versus the temperature. The expected C/H ratio of 0.46 is fully recovered at 1,200 K suggesting that the mass balance is conserved. At this initial temperature, seven species were observed, with their photoionization cross sections well defined. The precursor is 40% depleted, and most of carbon and hydrogen elements are still counted from *n*-dodecane. Thus the mass balance is well

conserved. As the temperature rises, the C/H ratios are a little higher than the expected ratio of 0.46. But the theoretical value of 0.46 is still completely covered within the error bars in the entire temperature range.

5. COMPUTATIONAL RESULTS

The *n*-dodecane molecule can decompose by initial cleavage of various C-C (reaction (R1)) and C-H bonds (reaction (R2)) producing pairs of 1-alkyl radicals and *n*-dodecyl radicals plus a hydrogen atom, respectively.



5.1. Homolytic C-C and C-H Bond Cleavages & Consecutive β -Scissions (C-C; C-H)

The energetics of the C-C bond cleavages in $\text{C}_{12}\text{H}_{26}$ is illustrated in Figure 5. The C-C bond strengths are calculated to be in the range of 361-366 kJ/mol, where the C2-C3 bond was found to be the weakest and the C5-C6 bond to be the strongest. The differences in the C-C bond strengths are so small that one can anticipate that all product pairs, $\text{CH}_3 + \text{C}_{11}\text{H}_{23}$, $\text{C}_2\text{H}_5 + \text{C}_{10}\text{H}_{21}$, $\text{C}_3\text{H}_7 + \text{C}_9\text{H}_{19}$, $\text{C}_4\text{H}_9 + \text{C}_8\text{H}_{17}$, $\text{C}_5\text{H}_{11} + \text{C}_7\text{H}_{15}$, and $\text{C}_6\text{H}_{13} + \text{C}_6\text{H}_{13}$, can be in principle formed. On the other hand, the calculated strengths of C-H bonds are significantly higher (Fig. 5). The primary C1-H bonds in terminal CH_3 groups are the strongest, 418 kJ/mol, whereas the secondary C-H bonds in CH_2 groups vary in a very narrow range of 406-407 kJ/mol. These values are close to the corresponding experimental C-C and C-H bond strengths in *n*-butane, propane, and ethane evaluated based on enthalpies of formation at 0 K from Active Thermochemical Tables⁸³ and also to the theoretical values for *n*-decane calculated in our previous work.⁴⁵

Due to the large difference in the bond strengths, rate constants for the C-H cleavages appeared to be several orders of magnitude lower than those for the C-C cleavages and therefore the C-C bond cleavage is predicted to dominate the unimolecular decomposition of dodecane (Figure 6(a)). In the temperature range of 1,000-1,600 K and 1 atm, the rate constants for the C-C cleavages exhibit well-defined Arrhenius behavior and grow from 2.6-3.6 s^{-1} to $1\text{-}2 \times 10^6 \text{ s}^{-1}$. These values agree with the experimental observations that while only a small fraction of *n*-dodecane is consumed at 1,100 K, no parent molecules survive above 1,500 K during the residence time in the reactor, about tens of microseconds. The computed rate constants for the

cleavages of the terminal bonds to produce $\text{CH}_3 + \text{C}_{11}\text{H}_{23}$ are found to be one-two orders of magnitude lower than those for the cleavage of non-terminal C-C bonds. The rate constants calculated at 1 atm, except for the one to produce $\text{CH}_3 + \text{C}_{11}\text{H}_{23}$, grow to $4\text{-}6 \times 10^7 \text{ s}^{-1}$ at 2,500 K; a small fall-off behavior at higher temperatures is seen in a decrease of the slope of the rate constant curves (Fig. 6(a)). The computed relative product yields are ~1% for $\text{CH}_3 + \text{C}_{11}\text{H}_{23}$, 17-16% for $\text{C}_2\text{H}_5 + \text{C}_{10}\text{H}_{21}$, 23-24% for $\text{C}_3\text{H}_7 + \text{C}_9\text{H}_{19}$, ~19% for $\text{C}_4\text{H}_9 + \text{C}_8\text{H}_{17}$, 18-19% for $\text{C}_5\text{H}_{11} + \text{C}_7\text{H}_{15}$, and 21-22% for $\text{C}_6\text{H}_{13} + \text{C}_6\text{H}_{13}$ and show very slight temperature dependence from 1,000 to 2,500 K. The product yields are also practically independent of pressure in the range from 30 Torr to 100 atm. This allows us to conclude that the pyrolysis of *n*-dodecane at 1,500 K and above should predominantly produce a mixture of 1-alkyl radicals, from ethyl to 1-decyl, on the timescale of 1-2 μs .

In our previous work considering the pyrolysis of *n*-decane⁴⁵ we have shown that the higher 1-alkyl radicals are unstable in the experimental temperature range and are subject to a rapid C-C bond β -scission producing ethylene C_2H_4 together with a smaller 1-alkyl. As shown in Fig. 5 and Table 6, the calculated barrier heights and reaction energies for the C-C bond β -scissions are 123-126 and 86-92 kJ/mol, respectively. The computed rate constants for C-C bond β -scissions are approximately in the range of $10^7\text{-}10^8 \text{ s}^{-1}$ at $T = 1,200\text{-}1,600 \text{ K}$ and hence, the lifetimes of the primary dissociation products, 1-alkyl radicals, is shorter than 1 μs under the experimental conditions and they are expected to rapidly decompose to the ultimate C_2H_4 , CH_3 , and C_2H_5 products detected experimentally via the stepwise mechanism shown below. Depending on the residence time, the ethyl radical may or may not further lose an H atom via a C-H bond β -scission producing ethylene.





The mechanism of consecutive direct C-C bond β -scissions unzipping large 1-alkyl radicals down to the mixture of C_2H_4 , C_2H_5 , and CH_3 cannot explain the experimental observation of higher 1-alkenes, especially propene and 1-butene, which are among major pyrolysis products at 1,200 K and are still present up to 1,600 K. We discussed several possible formation pathways of 1-alkenes in the previous paper on *n*-decane.⁴⁵ The first one is C-H bond β -scission in 1-alkyls, but according to the calculations C-H β -scission barriers are 20-26 kJ/mol higher than the corresponding C-C β -scission barriers in C_3H_7 - C_8H_{17} . Because of this difference, the computed branching ratios for the C-H β -scission channels in C_4H_9 - C_8H_{17} are very small and do not exceed 1-2% until the highest temperatures and pressures (2,500 K and 100 atm), where they reach 5-6%.⁴⁵ The relative yield of propene + H is higher from C_3H_7 and increases from 3-4% at 1,100-1,600 K and 1 atm to 6%, 9%, and 13% at 2500 K and pressures of 1, 10, and 100 atm, respectively. Thus, C-H bond β -scissions cannot explain the large experimental yields of propene and 1-butene since they are largely unfavorable compared to the β -scissions with the loss of C_2H_4 . **Summarizing, C-C bond cleavages leading to 1-alkyl radicals are strongly favored compared to C-H bond rupture processes; the higher 1-alkyl radicals (> C2) do not survive under our experimental conditions and decay via successive C-C β -scissions (C_2H_4 elimination), which dominate over C-H β -scission (alkene formation), to yield eventually the C1 to C2 hydrocarbons CH_3 , C_2H_5 , and C_2H_4 .**

5.2. Hydrogen Migrations & Consecutive β -Scissions

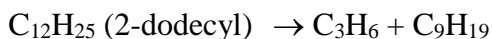
The second possible mechanism to form higher alkenes involves H atom shifts in 1-alkyl radicals followed by C-C bond β -scission. We have shown⁴⁵ that isomerization channels involving 1,2- and 1,3-H atom shifts in C_3H_7 and C_4H_9 are not competitive due to their high barriers of 157-162 kJ/mol significantly exceeding the C-C bond β -scission barriers of ~124 kJ/mol. On the other hand, a possibility of 1,4-H, 1,5-H, 1,6-H, and 1,7-H shifts eventually opens up in higher 1-alkyl radicals beginning from C_5H_{11} and the corresponding typical barriers for these processes, 92-94, 64-66, 71-72, and 80 kJ/mol, respectively, are *lower* than those for the C-C bond β -scission. The hydrogen shifts are followed by C-C β -scissions forming higher 1-alkenes rather than ethylene, i.e., propene (C_3H_6), 1-butene (C_4H_8), 1-pentene (C_5H_{10}), and so on,

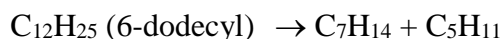
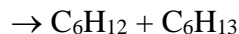
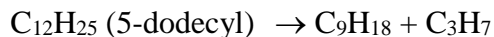
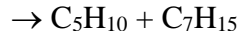
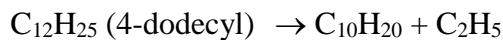
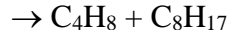
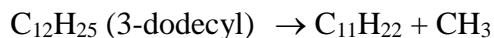
depending on the radical position in the alkyl. We calculated and reported product branching ratios in dissociation of 1-alkyl radicals C_5H_{11} - C_8H_{17} taking into account direct C-C and C-H β -scissions as well as all C-C β -scissions following the H shifts in the previous work⁴⁵ and demonstrated that at low pressures up to 1 atm, the products formed after a 1,5-H shift are preferable, but at high pressures of 10 and 100 atm, the direct C-C β -scission from 1-alkyls producing ethylene (C_2H_4) dominates. Nevertheless, various alkenes can be formed from the 1-alkyl radicals with non-negligible branching ratios, e.g., from C_5H_{11} : $C_3H_7 + C_2H_4$ (direct), $C_2H_5 + C_3H_6$ (via 1,4-H shift and 2-pentyl); from C_6H_{13} : $C_4H_9 + C_2H_4$ (direct), $C_3H_7 + C_3H_6$ (via 1,5-H shift and 2-hexyl), $CH_3 + C_5H_{10}$ and $C_2H_5 + C_4H_8$ (both via 1,4-H shift and 3-hexyl); etc. (see Figure 7 for the full list of possible products from 1-alkyls C_3H_7 - $C_{10}H_{21}$). As compared with *n*-decane, *n*-dodecane has two higher 1-alkyl radicals among its primary products, 1-nonyl (C_9H_{19}) and 1-decyl ($C_{10}H_{21}$). While one can expect that the barriers for 1,4-, 1,5-, 1,6-, and 1,7-H shifts should retain their typical values in C_9H_{19} and $C_{10}H_{21}$ and hence the corresponding H shift/C-C β -scission channels would remain competitive, new reaction channels may additionally open up, 1,8-H shifts both in 1-nonyl and 1-decyl and 1,9-H shift in 1-decyl. Here, we evaluated the 1,8- and 1,9-H shift barriers in $C_{10}H_{21}$. The calculation gave the values of 97 and 90 kJ/mol, respectively. While these barriers are higher than those for 1,5-, 1,6-, and 1,7-H shifts, and are comparable to 1,4-H shifts, they are still somewhat lower than the barrier for the direct C-C β -scission. Therefore, the dissociation channels involving the 1,8- and 1,9-H shifts followed by C-C β -scissions can give minor contributions to the overall product yield. In particular, 1-nonyl can isomerize to 2-nonyl by 1,8-H shift and then decompose to $C_6H_{13} + C_3H_6$. 1-decyl can isomerize to 2-decyl by 1,9-shift and dissociate to $C_7H_5 + C_3H_6$ or isomerize to 3-decyl and decompose to either $CH_3 + C_9H_{18}$ or $C_6H_{13} + C_4H_8$. **Summarizing, the reaction mechanism involving hydrogen migration in C5 to C10 1-alkyl radicals preceding C-C β -scission accounts for the observation of C3-C7 alkenes [propene, 1-butene, 1-pentene, 1-hexene, and 1-heptene] observed in our experiments, and especially, for the large branching ratios of C_3H_6 and C_4H_8 at low temperatures (and even at 1,600 K for propene). At temperatures of 1,500 K and above the lifetime of a single C-C bond approaches 1 μ s and hence higher alkenes are likely to decompose on the timescale of the experiment and their yield significantly decrease.**

5.3. Hydrogen Abstraction

The third possible pathway to the higher alkenes involves C-C bond β -scissions in *n*-dodecyl radicals ($n > 1$, see Fig. 5 and Table 6). While *n*-dodecyls are not expected to be formed by C-H bond cleavages in *n*-dodecane, they can be produced by direct hydrogen abstractions by H atoms or other radicals when those radicals appear in the reactive system. The barrier heights and reaction exoergicities for the H abstraction reactions by a hydrogen atom from secondary C-H bonds are computed to be 35-36 (27-28) and 23-24 (30-31) kJ/mol; the numbers in parenthesis include HLC in the G3(CCSD,MP2) calculations. The H abstractions from the primary C-H bonds exhibit a higher barrier and a lower reaction exoergicity of 49 (42) and 12 (19) kJ/mol, respectively. These results are close to the corresponding values obtained in the previous work for *n*-decane.⁴⁵ Note that, the most accurate up-to-date calculations of H abstraction from C₃H₈ and C₂H₆ gave the reaction barriers and exoergicities as 32 and 27 kJ/mol, respectively, for the secondary hydrogen abstraction and 43-44 and 15-16 kJ/mol for the primary hydrogen abstraction.⁸⁴ The calculated rate constants for secondary H abstractions are generally higher than those for the primary hydrogen abstraction (Fig. 6(b)) and, among secondary H abstractions, the reaction producing 5-dodecyl is preferred and followed by the reactions giving 5-dodecyl, then by 2- and 3-dodecyl (with similar rate constants), and finally by 4-dodecyl. The computed rate constants to form 2- and 3-dodecyl agree best with the literature data (the most accurate calculations for C₃H₈⁸⁴ and experimental data for C₃H₈, C₄H₁₀, and C₅H₁₂⁸⁵⁻⁸⁶) for the secondary H abstraction at 500 K but overestimate the literature data at 2,500 K by approximately a factor of 3. Alternatively, the rate constants for the production of 4-dodecyl agree closely with the literature values at high temperatures. Our results indicate that the rate constants for secondary H abstraction are sensitive to the attacked hydrogen atom position in the alkane. It should be noted however that a more rigorous anharmonic treatment of soft normal modes would be required to generate quantitatively accurate H abstraction rate constants. For the primary hydrogen abstraction, the C₁₂H₂₆ + H rate constants underestimate those for C₃H₈ + H by 50-60% if HLC is taken into account; the difference is bigger if the correction is not included.

Our main conclusion is that the secondary H abstractions are feasible and form *n*-dodecyl radicals ($n > 1$). Once the *n*-dodecyl radicals are produced, they can rapidly undergo C-C bond β -scission to yield higher alkenes together with 1-alkyl radicals:





The calculated barriers for these reactions are 123-125 kJ/mol and they are endoergic by 88-93 kJ/mol; these energetic parameters are thus similar to those for C-C β -scissions in smaller alkyl radicals considered above and in the previous work.⁴⁵ The rate constants calculated at 1 atm are close for all the reactions considered within a factor of 2 (Fig. 6(c)). The results indicate that the lifetime of the dodecyl varies in the 5-50 ns range under the experimental conditions. **Summarizing, n-dodecyl radicals, which may be produced by hydrogen abstraction, can also undergo subsequent C-C bond β -scissions leading to experimentally observed alkenes: 1-butene, 1-pentene, 1-hexene, and 1-heptene.**

6. DISCUSSION & CONCLUSION

We combine now the experimental results with the electronic structure and rate constant calculations with the goal to elucidate the (predominant) temperature-dependent decomposition pathways. The compiled mechanism of the pyrolysis is illustrated in Figures 7 and 8.

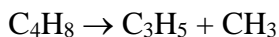
1. At the initial stage, *n*-dodecane dissociates by C-C bond cleavages (excluding the terminal C-C bonds) and produces $\text{C}_{10}\text{H}_{21} + \text{C}_2\text{H}_5$, $\text{C}_9\text{H}_{19} + \text{C}_3\text{H}_7$, $\text{C}_8\text{H}_{17} + \text{C}_4\text{H}_9$, $\text{C}_7\text{H}_{15} + \text{C}_5\text{H}_{11}$, and $\text{C}_6\text{H}_{13} + \text{C}_6\text{H}_{13}$, i.e., a mixture of C2 to C10 1-alkyl radicals from ethyl to 1-decyl.

2. The alkyl radicals are unstable under the experimental conditions. They rapidly dissociate by two possible mechanisms: a) C-C bond β -scissions to split ethylene (C_2H_4) plus a 1-alkyl radical with the number of carbon atoms reduced by two and b) 1,4-, 1,5-, 1,6-, 1,7-, 1,8-, or 1,9-H shifts followed by C-C β -scission producing alkenes from propene to 1-nonene in combination with smaller 1-alkyl radicals. The higher alkenes become increasingly unstable as the temperatures rises and the yield of propene and 1-butene, large at 1,200 K, decreases. When the C-C β -

scission continues all the way to the propyl radical, C₃H₇, it dissociates producing CH₃ + C₂H₄. This mechanism allows us to explain the appearance of the predominant pyrolysis products, ethylene (C₂H₄), methyl (CH₃), ethyl (C₂H₅), propene (C₃H₆), and 1-butene (C₄H₈), as well as small yields of 1-pentene (C₅H₁₀), 1-hexene (C₆H₁₂), and 1-heptene (C₇H₁₄). The higher yield of the ethyl radical here as compared to *n*-decane may be related to the fact that a larger amount of higher 1-alkyl radicals is formed among the primary decomposition products of *n*-dodecane. These higher 1-alkyls require more C-C β-scission steps and hence a longer time to reach C₂H₅. Consequently, a larger fraction of the C₂H₅ radicals survives and does not dissociate to C₂H₄ + H before leaving the reactor.

3. At higher temperatures, hydrogen atoms can abstract hydrogen from C₁₂H₂₆ to yield *n*-dodecyl radicals. The *n*-dodecyl radicals can dissociate via C-C bond β-scissions to C₃-C₁₁ alkenes. Hydrogen migration and β-scissions of radicals are important reactions in hydrocarbon decomposition.⁸⁷⁻⁸⁸

4. The other trace products, which account for a maximum of about 10%, can only be produced via higher order reactions. For instance, acetylene C₂H₂ can be formed via unimolecular decomposition of C₂H₄ by sequential losses of two H atoms or by H₂ elimination.⁸⁹ In contrast to the *n*-decane pyrolysis,⁴⁵ we have not observed the vinyl radical C₂H₃ here, although it can be in principle formed by H loss from C₂H₄ or via a single C-C bond cleavage in higher alkenes. Apparently, the yield of C₂H₃ is too low for this radical to be detected in this work. The allyl radical C₃H₅ can be formed by the primary C-H bond cleavage in propene or a single C-C bond cleavage in higher alkenes:



The allyl radical is well known to eventually decompose to allene, methylacetylene (C₃H₄) and eventually to the propargyl radical C₃H₃.⁹⁰⁻⁹² Propargyl was not detected in the present experiment indicating that its yield was too small. At last, 2-butene can be formed by isomerization of 1-butene⁹³ and 1,3-butadiene is a major dissociation product of the C₄H₇

radical,⁹⁴ which in turn can be produced by C-H bond cleavage in 1-butene⁹² or by C-C bond cleavage in higher alkenes starting from 1-pentene.

Comparing the results of the present experiment with those from previous experimental studies, it should be noted that the earlier investigations were mostly limited to the identification of closed-shell hydrocarbon intermediates and products because the decomposition products were derived mainly from off-line and *ex situ* (HPLC, GC MS) analysis. This approach disallowed the detection of thermally unstable intermediates and hydrocarbon radicals. This limitation has been overcome in the present investigation since photoionization of the decomposition products on-line and *in situ* is a solid and versatile experimental tool allowing the detection of a full set of decomposition products including both thermally stable and unstable species, such as radicals. Additionally, we observed the decomposition products on the microsecond time scale, meaning that the initial decomposition products were detected. In previous experiments in the reactors and shock tubes, residence timescales were in the order of a few milliseconds (Table 1) and thermally unstable products, especially, radicals are not likely to survive, although they may have been formed initially. Therefore, the present study provides a most complete record of radicals and other thermally unstable species produced in the initial stage of decomposition and thus de facto characterizes the radical pool available for further oxidation of the fuel, which is required for generation of accurate kinetic models of combustion of aviation fuels. Also, the short residence time used in the present work effectively excludes undesired mass growth processes. Finally, the combined experimental and theoretical studies of *n*-dodecane and earlier,⁴⁵ of *n*-decane allowed us to reveal and clearly formulate the chemical mechanism of the pyrolysis of large *n*-alkane molecules, which represent the major fuel components.

AUTHOR INFORMATION

Corresponding Authors

Email: ralfk@hawaii.edu.

Email: MAhmeed@lbl.gov.

Email: mebela@fiu.edu.

Notes

The authors declare no competing financial interest.

Supporting Information.

Table S1. Detected molecules in previous experimental studies of *n*-dodecane pyrolysis. **Table S2.** Parameters of the fitted modified Arrhenius expressions, $A \cdot T^\alpha \cdot \exp(-E_a/RT)$, for most important reactions involved in pyrolysis of *n*-dodecane at pressures of 0.03-0.04, 1, 10, and 100 atm.

ACKNOWLEDGMENTS

This project is supported by the Air Force Office of Scientific Research (AFOSR) under Grant Number FA9550-15-1-0011 (L. Z., T. Y., R. I. K., A. M. M.) to the University of Hawaii and Florida International University. T. P. T. and M. A. along with the Advanced Light Source are supported by the Director, Office of Science, Office of Basic Energy Sciences, of the U.S. Department of Energy under Contract No. DE-AC02-05CH11231, through the Chemical Sciences Division.

Table 1. Compilation of previous experimental studies on the pyrolysis of *n*-dodecane.

Group	Method	Temperature (K)	Pressure (atm)	Residence time (ms)	Ref.
Brezinsky	High-pressure shock tube	867-1,739	22.84, 49.42	1.15-3.47	³⁰
Davidson	Shock tube	990-1520	17-23	2	³¹
Banerjee	Flow reactor	1,000-1,300	1	0-40	³²
Bounaceur	Flow reactor	950, 1,000 and 1,050	1	200	³³
Herbinet	JSR	773-1073	1	1,000-5,000	³⁴
Zhou	Flow reactor	623-893	1	3,300-12,300	³⁵
Eser	Stainless steel tubing bomb reactor	673-723	10-100	9.0E8-3.6E9	³⁶⁻³⁷

Table 2. Compilation of products observed in the present experiments on the decomposition of *n*-dodecane.

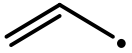
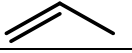

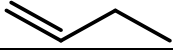

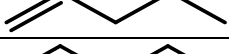
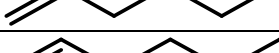
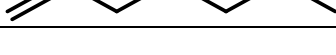
Molecule	Formula	Mass	Structure
Hydrogen	H ₂	2	H—H
Methyl radical	CH ₃	15	CH ₃ •
Acetylene	C ₂ H ₂	26	≡≡
Ethylene	C ₂ H ₄	28	≡≡
Ethyl radical	C ₂ H ₅	29	—•
Allene	C ₃ H ₄	40	≡C≡
Methylacetylene	C ₃ H ₄	40	≡—
Allyl radical	C ₃ H ₅	41	
Propene	C ₃ H ₆	42	
1,3-Butadiene	C ₄ H ₆	54	
1-Butene	C ₄ H ₈	56	
2-Butene	C ₄ H ₈	56	
1-Pentene	C ₅ H ₁₀	70	
1-Hexene	C ₆ H ₁₂	84	
1-Heptene	C ₇ H ₁₄	98	

Table 3. Branching fractions of the products in the decomposition of *n*-dodecane at 600 Torr in the chemical reactor at 1,200, 1,300, 1,400, 1,500 K and 1,600 K.

Species*	Formula	Mass	Temperature				
			1,200 K	1,300 K	1,400 K	1,500 K	1,600 K
Hydrogen	H ₂	2	-	6.63±1.99	3.68±0.97	4.95±1.15	11.40±3.22
Methyl radical	CH ₃	15	10.41±3.60	9.38±2.32	11.63±2.53	13.15±2.87	9.01±2.41
Acetylene	C ₂ H ₂	26	-	-	-	0.23±0.06	1.59±0.36
Ethylene	C ₂ H ₄	28	29.85±7.99	40.44±8.71	52.35±11.82	57.67±13.03	60.28±13.50
Ethyl radical	C ₂ H ₅	29	20.46±6.32	8.68±2.20	3.35±0.80	0.85±0.28	-
Allene	C ₃ H ₄	40	-	-	0.55±0.18	2.74±0.67	5.37±1.16
Methylacetylene	C ₃ H ₄	40	-	-	-	0.52±0.34	1.32±0.86
Allyl radical	C ₃ H ₅	41	-	4.46±1.29	8.02±1.98	8.52±2.16	1.79±0.52
Propene	C ₃ H ₆	42	13.14±4.19	10.70±3.09	10.51±2.59	8.85±1.96	8.03±1.80
1,3-Butadiene	C ₄ H ₆	54	-	-	0.34±0.08	0.42±0.09	0.38±0.09
1-Butene	C ₄ H ₈	56	18.45±6.50	12.49±4.22	6.17±1.84	1.59±0.41	0.41±0.14
2-Butene	C ₄ H ₈	56	-	-	-	0.08±0.04	0.06±0.03
1-Pentene	C ₅ H ₁₀	70	3.95±1.56	3.01±0.83	1.53±0.40	0.18±0.05	-
1-Hexene	C ₆ H ₁₂	84	3.74±1.22	3.63±0.83	1.67±0.40	0.09±0.03	-
1-Heptene	C ₇ H ₁₄	98	0.15±0.07	1.00±0.16	0.71±0.09	-	-

***Note:** As there is no cross section database of 1-heptene, its branching fraction cannot be calculated. Therefore, the normalized ion count intensities of 1-heptene at 10.0 eV are listed in the last row to reveal the trend of 1-heptene formation from 1,200 to 1,600 K.

Table 4. The photoionization cross sections of the species at selected energies exploited for the calculations of the branching ratios in this work.

Species	Formula	Mass	Photon Energy (eV)						Ref.
			9.5	10.0	10.5	11.0	11.5	15.5	
Hydrogen	H ₂	2	-	-	-	-	-	4.73	95
Methyl radical	CH ₃	15	-	4.78	5.81	-	-	-	96
Acetylene	C ₂ H ₂	26	-	-	-	-	18.258	-	57
Ethylene	C ₂ H ₄	28	-	-	0.918	7.794	8.016	-	97
Ethyl radical	C ₂ H ₅	29	4.36	5.05	5.52	5.64	5.37	-	98
Allene	C ₃ H ₄	40	-	5.66	15.48	22.26	25.84	-	99
Methylacetylene	C ₃ H ₄	40	-	-	23.06	43.84	42.1	-	97
Allyl radical	C ₃ H ₅	41	5.636	6.227	6.091	-	-	-	100
Propene	C ₃ H ₆	42	-	5.33	9.05	11.40	12.66	-	101
1,3-Butadiene	C ₄ H ₆	54	8.48	13.96	16.44	19.91	22.45	-	99
1-Butene	C ₄ H ₈	56	-	7.35	10.02	10.88	17.33	-	101
2-Butene	C ₄ H ₈	56	5.24	9.06	11.04	14.05	19.17	-	102
1-Pentene	C ₅ H ₁₀	70	0.62	14.38	14.90	14.83	13.92	-	102
1-Hexene	C ₆ H ₁₂	84	0.89	8.58	9.65	8.86	9.00	-	99
<i>n</i> -dodecane	C ₁₂ H ₂₆	170	0.01	3.325	30.058	43.15	53.542	-	103

Table 5. The database and measured photoionization energies of the species in the PIE scan.

Species	Formula	Mass	Photoionization Energy (eV)					
			Database ⁷⁰	1,200 K	1,300 K	1,400 K	1,500 K	1,600 K
Methyl radical	CH ₃	15	9.839	9.85	9.75	9.75	9.75	9.75
Acetylene	C ₂ H ₂	26	11.4	-	-	-	11.3	10.35
Ethylene	C ₂ H ₄	28	10.514	10.40	10.50	10.50	10.45	10.45
Ethyl radical	C ₂ H ₅	29	8.117	8.15	8.15	8.10	8.10	-
Allene	C ₃ H ₄	40	9.692	-	-	9.70	9.75	9.70
Methylacetylene	C ₃ H ₄	40	10.36	-	-	-	10.30	10.30
Allyl radical	C ₃ H ₅	41	8.18	-	8.10	8.10	8.10	8.10
Propene	C ₃ H ₆	42	9.73	9.75	9.70	9.75	9.70	9.70
1,3-Butadiene	C ₄ H ₆	54	9.072	-	-	9.05	9.05	9.05
1-Butene	C ₄ H ₈	56	9.55	9.55	9.55	9.55	9.60	9.55
2-Butene	C ₄ H ₈	56	9.11	-	-	-	9.10	9.15
1-Pentene	C ₅ H ₁₀	70	9.49	9.55	9.50	9.45	9.55	-
1-Hexene	C ₆ H ₁₂	84	9.44	9.45	9.45	9.45	9.45	-
1-Heptene	C ₇ H ₁₄	98	9.27	9.30	9.30	9.30	-	-
<i>n</i> -dodecane	C ₁₂ H ₂₆	170	9.64*	9.65	9.65	9.65	-	-

***Note:** based on the cross section curve of *n*-dodecane, the ionization energy is about 9.64 eV.

Table 6. Calculated barrier heights and reaction energies for various C-C bond β -scission and direct H abstraction reactions.

Reactions	Barrier (kJ/mol)	Reaction energy (kJ/mol)
$C_{11}H_{23} \rightarrow C_9H_{19} + C_2H_4$	124	90
$C_{10}H_{21} \rightarrow C_8H_{17} + C_2H_4$	123	89
$C_9H_{19} \rightarrow C_7H_{15} + C_2H_4$	124	89
$C_8H_{17} \rightarrow C_6H_{13} + C_2H_4$	124	92
$C_7H_{15} \rightarrow C_5H_{11} + C_2H_4$	124	91
$C_6H_{13} \rightarrow C_4H_9 + C_2H_4$	124	89
$C_5H_{11} \rightarrow C_3H_7 + C_2H_4$	124	89
$C_4H_9 \rightarrow C_2H_5 + C_2H_4$	123	86
$C_3H_7 \rightarrow CH_3 + C_2H_4$	126	86
$C_{12}H_{25}$ (1-dodecyl) $\rightarrow C_{10}H_{21} + C_2H_4$	124	90
$C_{12}H_{25}$ (2-dodecyl) $\rightarrow C_9H_{19} + C_3H_6$	124	92
$C_{12}H_{25}$ (3-dodecyl) $\rightarrow C_{11}H_{22} + CH_3$	125	89
$C_{12}H_{25}$ (3-dodecyl) $\rightarrow C_8H_{17} + C_4H_8$	125	93
$C_{12}H_{25}$ (4-dodecyl) $\rightarrow C_{10}H_{20} + C_2H_5$	123	88
$C_{12}H_{25}$ (4-dodecyl) $\rightarrow C_5H_{10} + C_7H_{15}$	125	93
$C_{12}H_{25}$ (5-dodecyl) $\rightarrow C_9H_{18} + C_3H_7$	125	92
$C_{12}H_{25}$ (5-dodecyl) $\rightarrow C_6H_{12} + C_6H_{13}$	125	93
$C_{12}H_{25}$ (6-dodecyl) $\rightarrow C_7H_{14} + C_5H_{11}$	125	92
$C_{12}H_{25}$ (6-dodecyl) $\rightarrow C_8H_{16} + C_4H_9$	125	92
$C_{12}H_{26} + H \rightarrow C_{12}H_{25}$ (1-dodecyl) $+ H_2$	49 (42) ^a	-12 (-19) ^a
$C_{12}H_{26} + H \rightarrow C_{12}H_{25}$ (2-dodecyl) $+ H_2$	36 (28) ^a	-24 (-31) ^a
$C_{12}H_{26} + H \rightarrow C_{12}H_{25}$ (3-dodecyl) $+ H_2$	36 (28) ^a	-23 (-30) ^a
$C_{12}H_{26} + H \rightarrow C_{12}H_{25}$ (4-dodecyl) $+ H_2$	35 (28) ^a	-23 (-31) ^a
$C_{12}H_{26} + H \rightarrow C_{12}H_{25}$ (5-dodecyl) $+ H_2$	35 (27) ^a	-23 (-31) ^a
$C_{12}H_{26} + H \rightarrow C_{12}H_{25}$ (6-dodecyl) $+ H_2$	35 (27) ^a	-23 (-30) ^a

^aThe values including the higher level correction (HLC) for H abstractions are given in parenthesis.

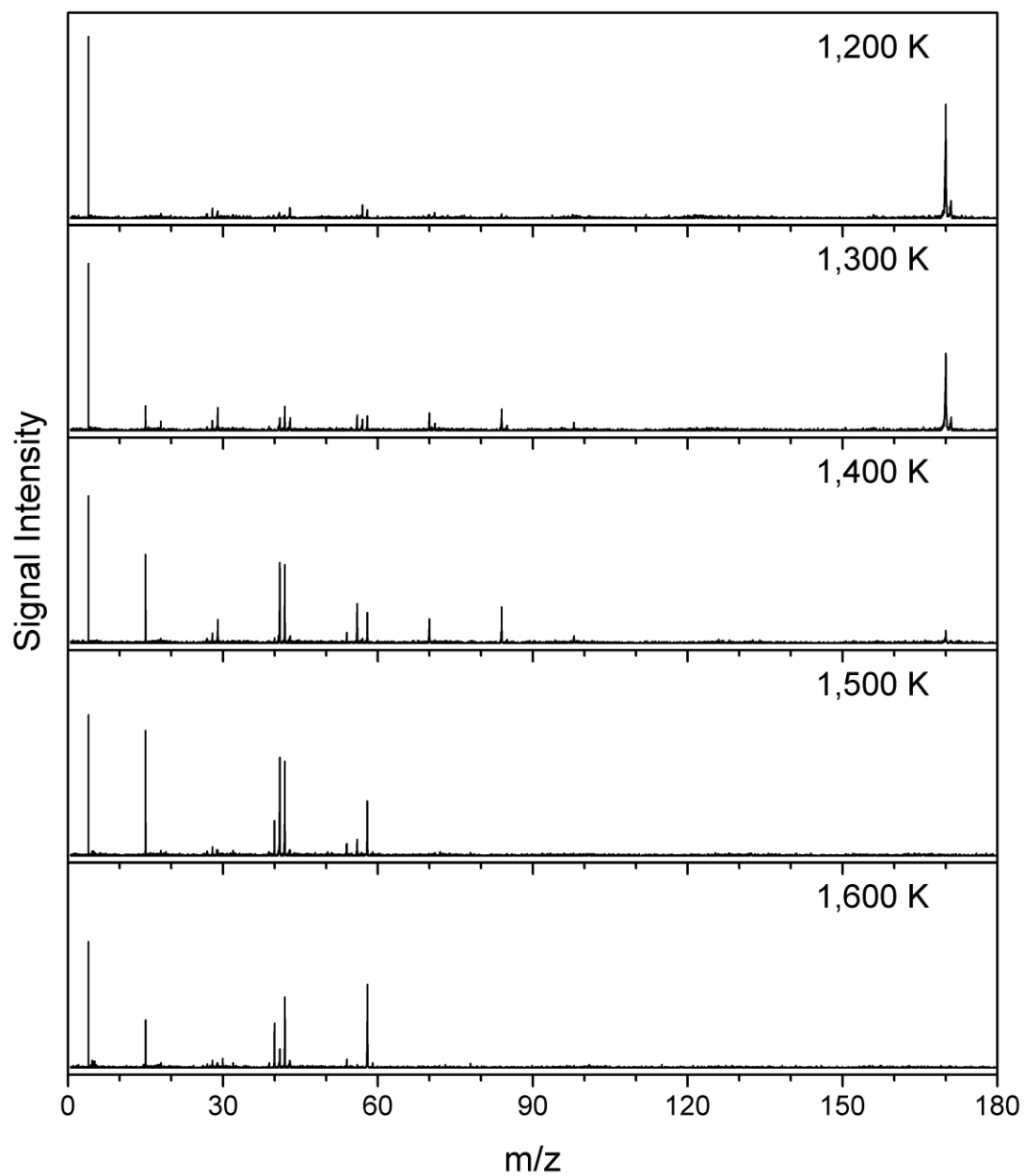


Figure 1. Mass spectra of the products obtained from the decomposition of *n*-dodecane recorded at a photon energy of 10.0 eV at different temperatures from 1,200 K to 1,600 K.

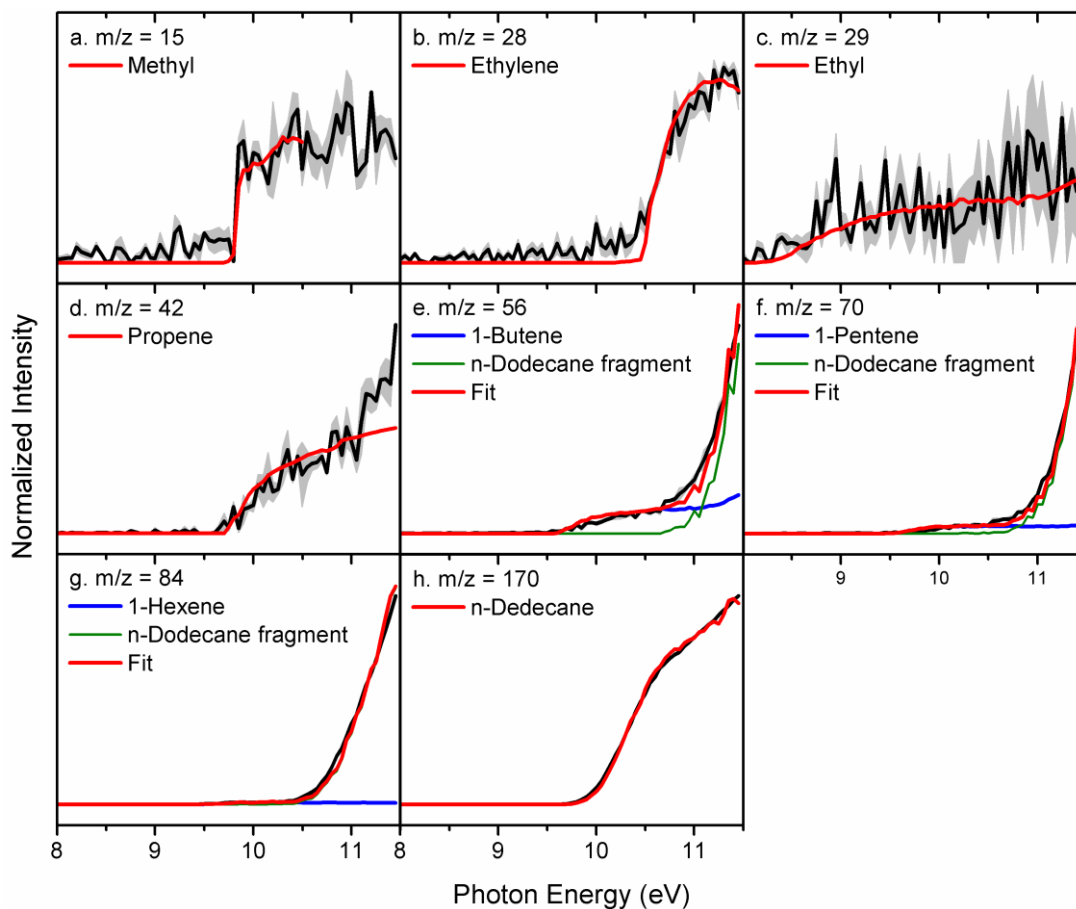


Figure 2-1. Experimental photoionization efficiency (PIE) curves (black lines) recorded from the decomposition of *n*-dodecane at 1,200 K along with the experimental errors (gray area) and the reference PIE curves (red, green and blue lines).

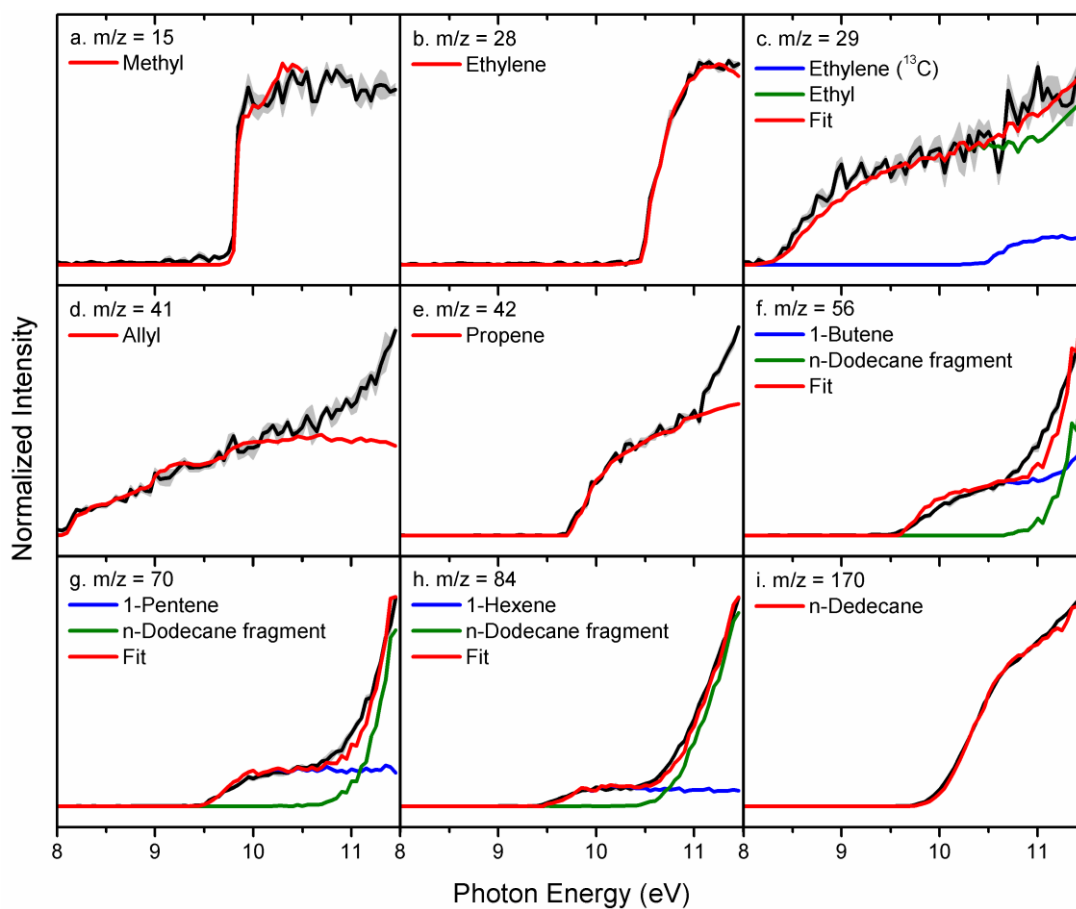


Figure 2-2. Experimental photoionization efficiency (PIE) curves (black lines) recorded from the decomposition of *n*-dodecane at 1,300 K along with the experimental errors (gray area) and the reference PIE curves (red, green and blue lines). For $m/z = 41$ and 42 , there may be some photoionization fragments from initial decomposition products causing the experimental values to be higher than the fittings at higher energies.

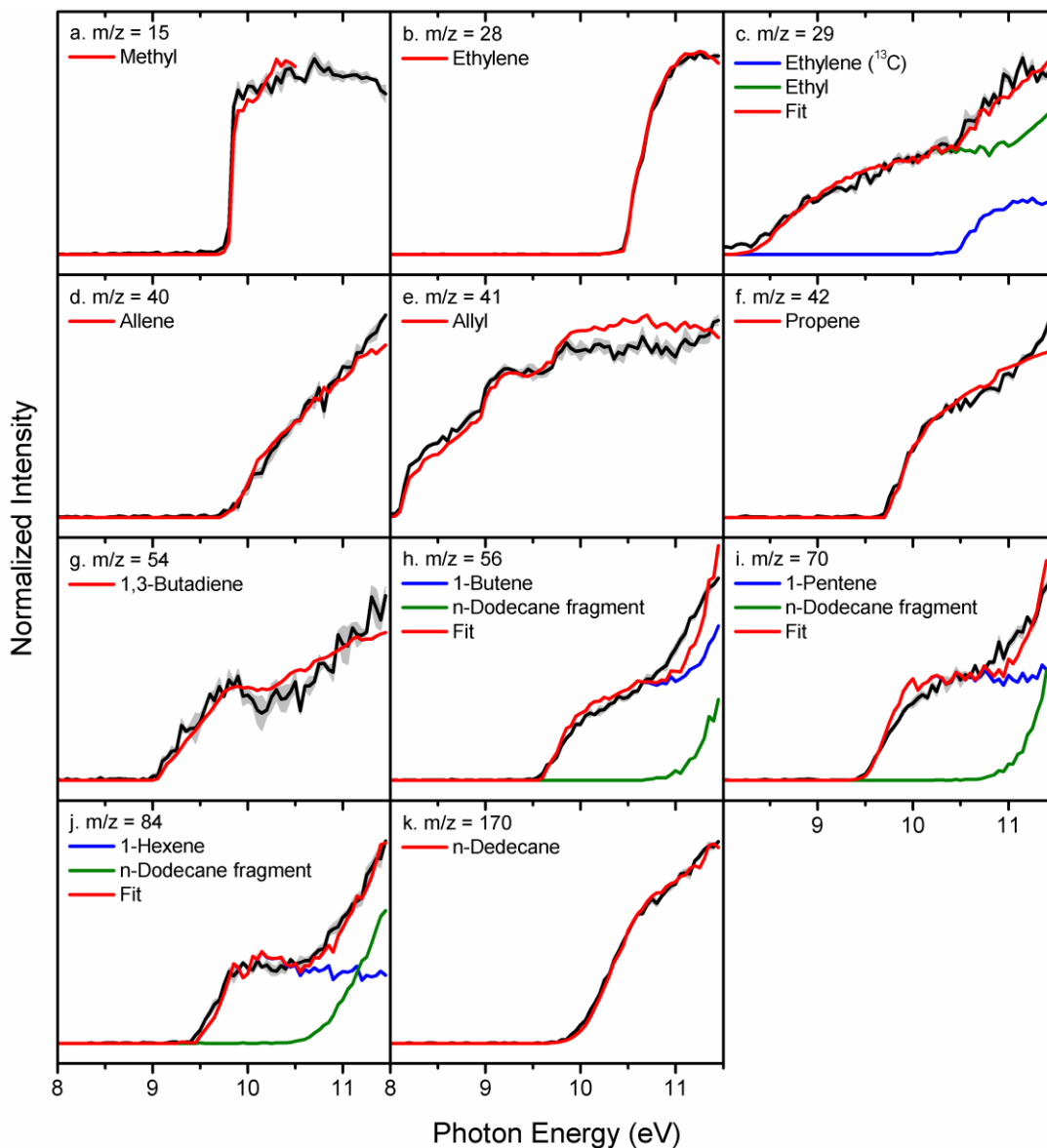


Figure 2-3. Experimental photoionization efficiency (PIE) curves (black lines) recorded from the decomposition of *n*-dodecane at 1,400 K along with the experimental errors (gray area) and the reference PIE curves (red, green and blue lines).

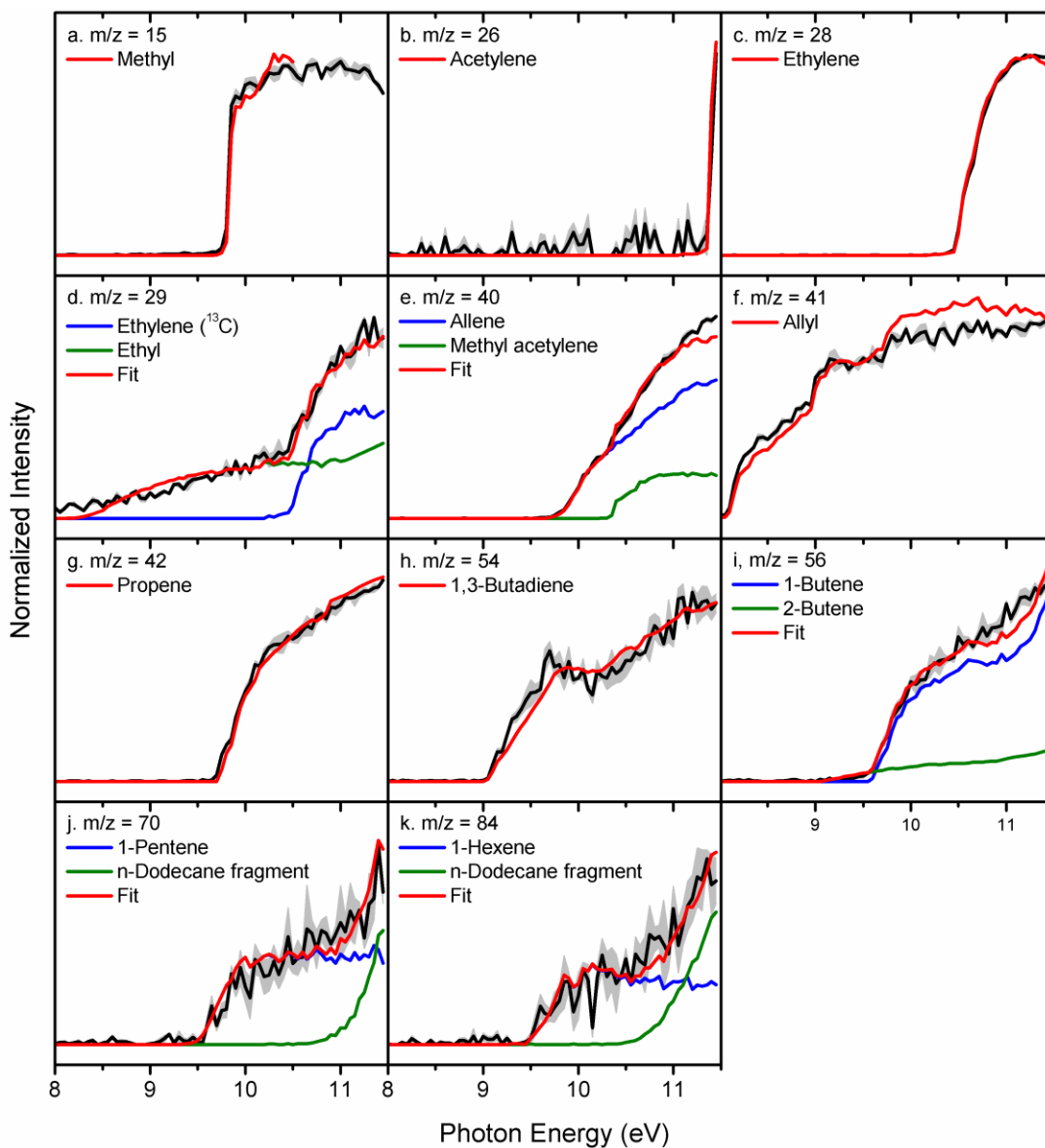


Figure 2-4. Experimental photoionization efficiency (PIE) curves (black lines) recorded from the decomposition of *n*-dodecane at 1,500 K along with the experimental errors (gray area) and the reference PIE curves (red, green and blue lines).

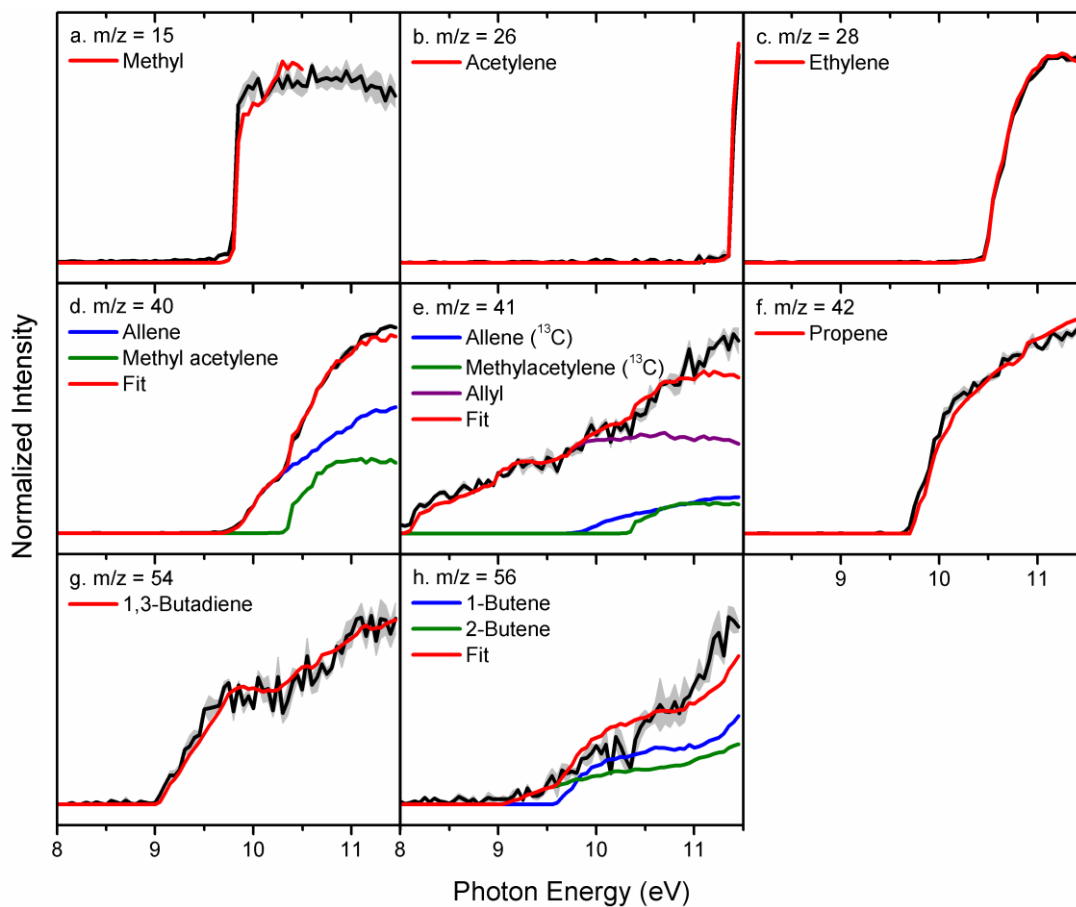


Figure 2-5. Experimental photoionization efficiency (PIE) curves (black lines) recorded from the decomposition of *n*-dodecane at 1,600 K along with the experimental errors (gray area) and the reference PIE curves (red, green and blue lines).

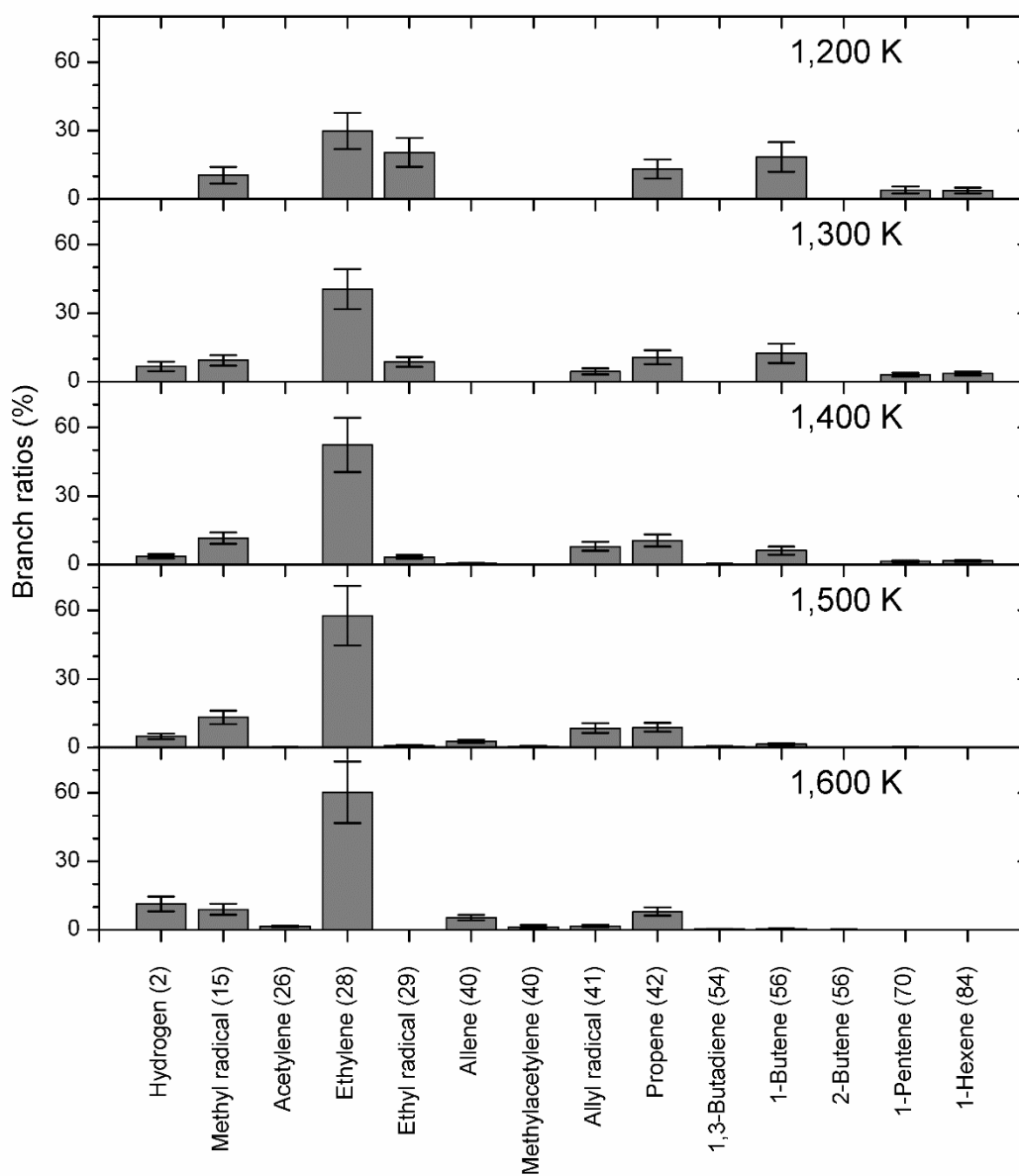


Figure 3. Overall branching ratios of the species obtained in the decomposition of *n*-dodecane in the temperature range from 1,200 to 1,600 K.

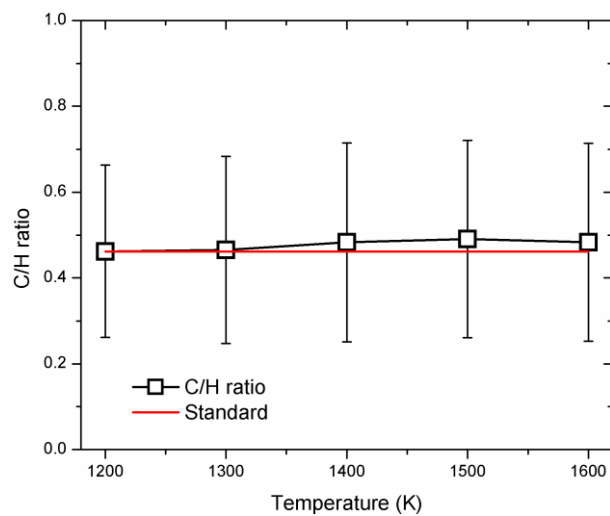


Figure 4. Carbon-to-hydrogen (C/H) ratios in the decomposition of *n*-dodecane in the temperature range from 1,200 to 1,600 K. Red line defines the standard C/H ratio of *n*-dodecane.

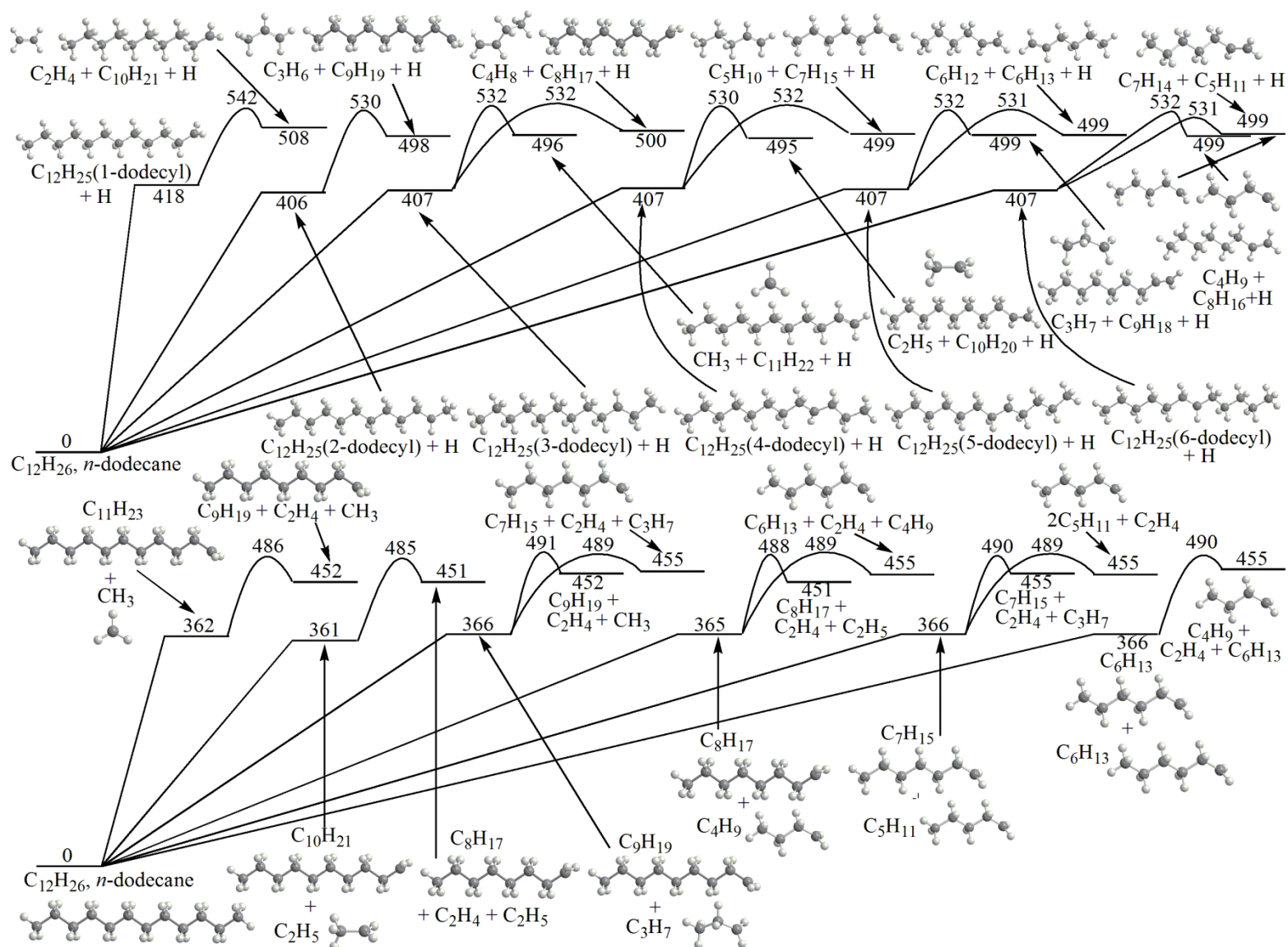


Figure 5. Potential energy diagram for primary and secondary dissociation channels of *n*-dodecane. All relative energies are shown in kJ/mol.

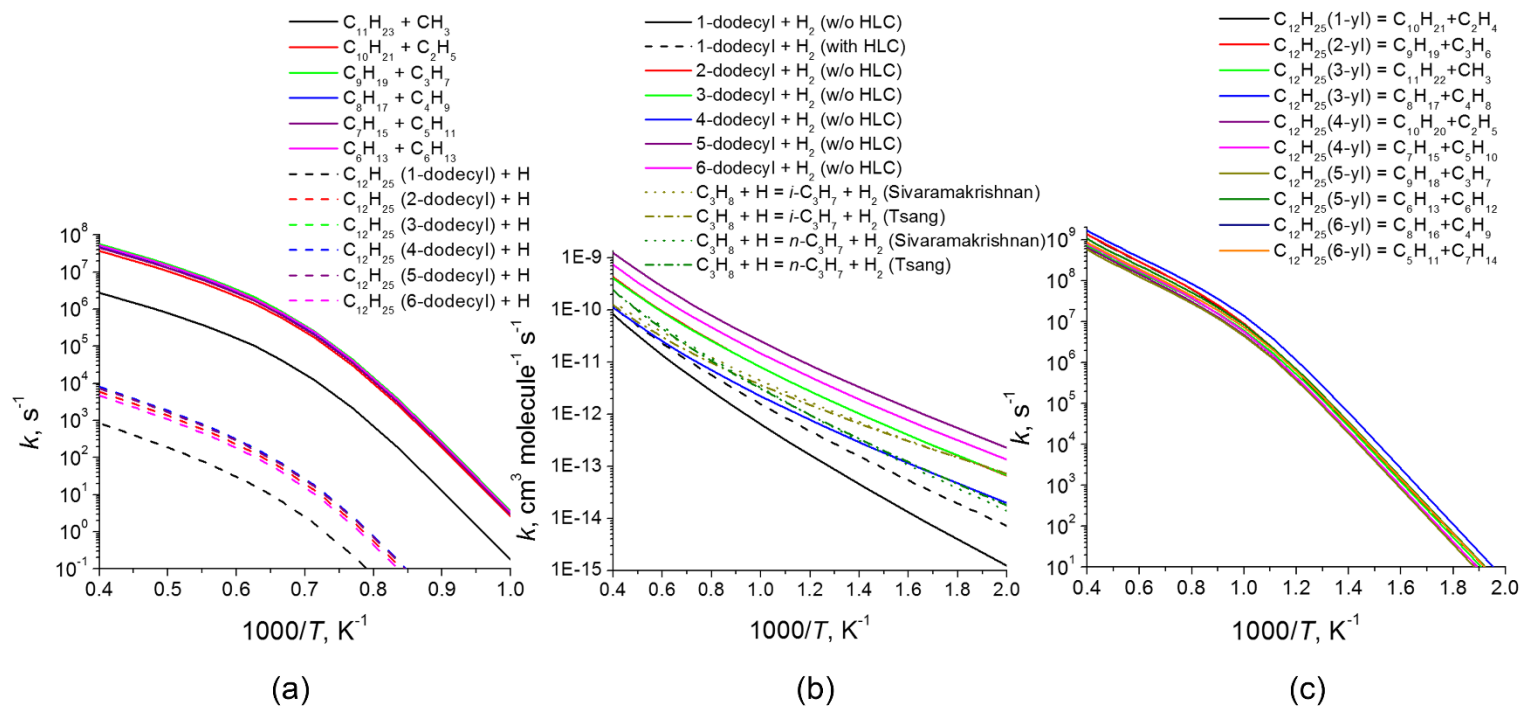


Figure 6. Calculated rate constants (at 1 atm for unimolecular reactions): (a) for C-C and C-H bond cleavages in $\text{C}_{12}\text{H}_{26}$; (b) for $\text{C}_{12}\text{H}_{26} + \text{H}$ direct H abstractions; and (c) for C-C bond β -scissions in n-dodecyl radicals $\text{C}_{12}\text{H}_{25}$ ($n = 1-6$).

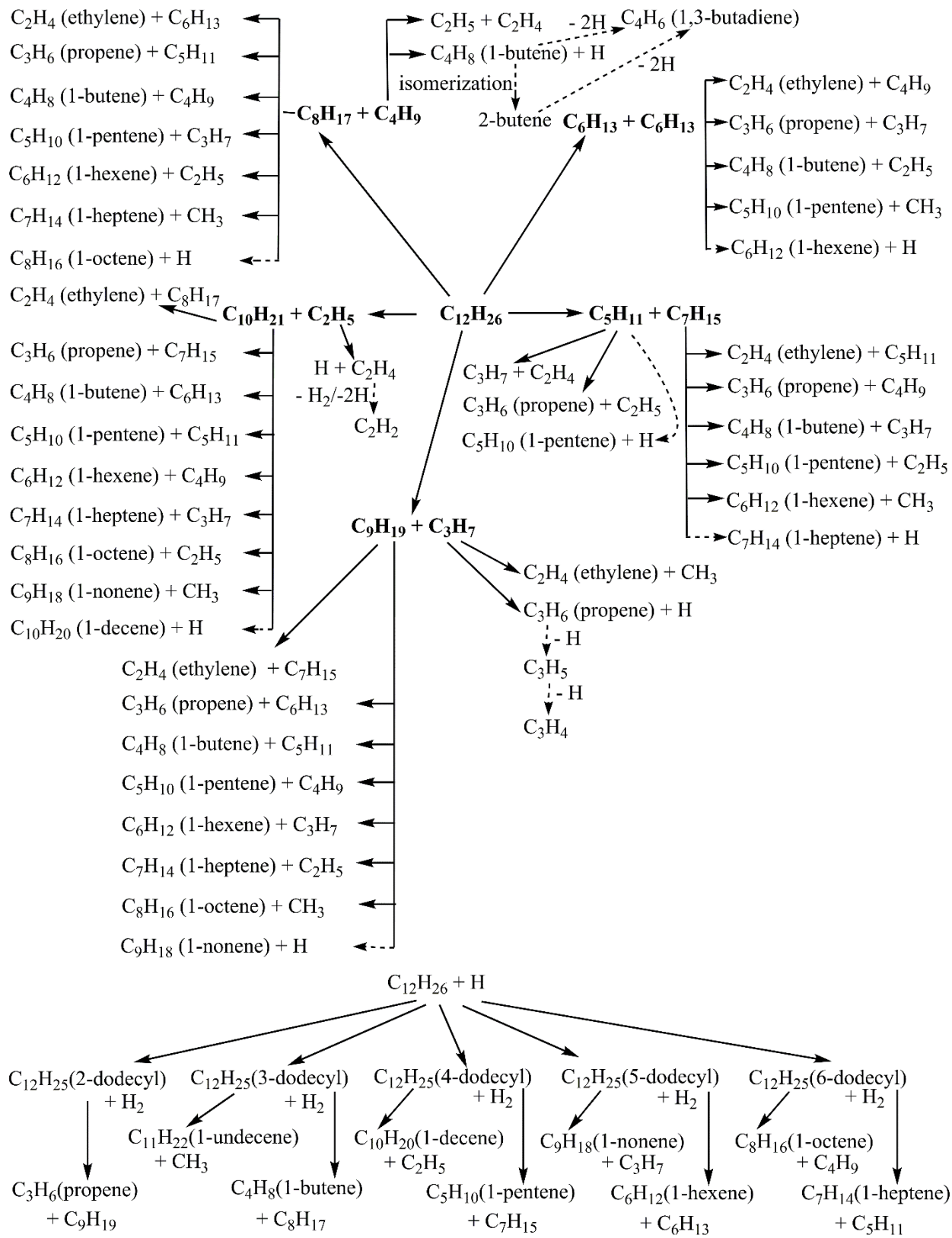


Figure 7. Proposed reaction mechanism for the pyrolysis of *n*-dodecane.

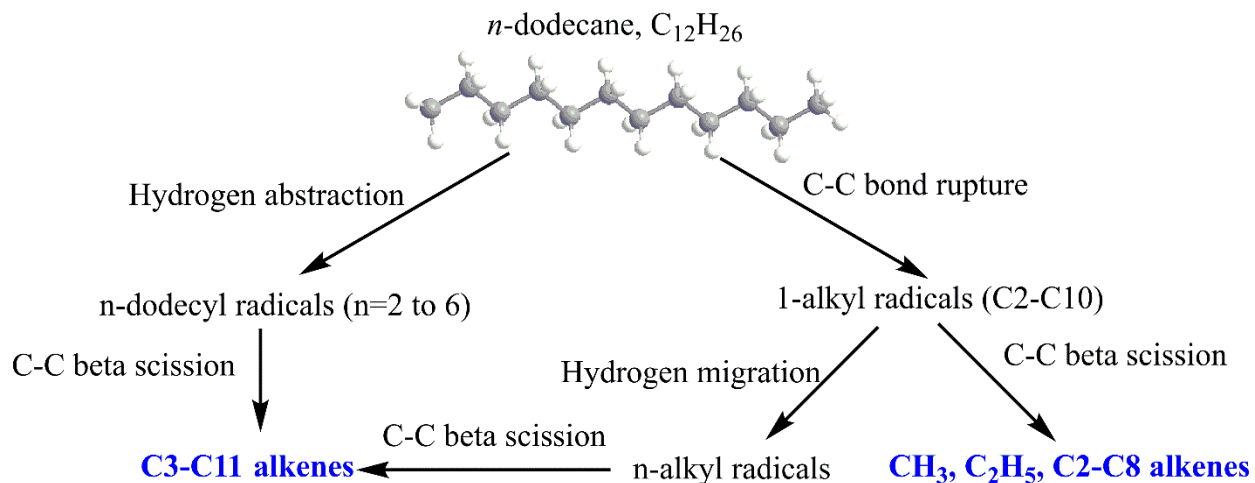


Figure 8. Summary of reaction mechanisms leading to primary reaction products in the decomposition of *n*-dodecane.

References

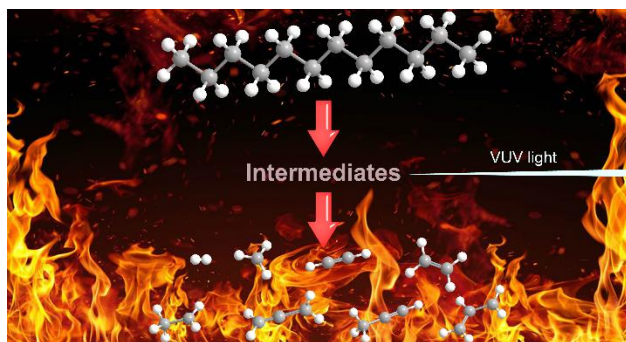
- (1) Bruno, T. J.; Abel, K. R.; Riggs, J. R. Comparison of JP-8 and JP-8+100 with the Advanced Distillation Curve Approach. *Energy Fuels* **2012**, *26*, 5843-5850.
- (2) Bezaire, N.; Wadumesthrige, K.; Simon Ng, K. Y.; Salley, S. O. Limitations of the Use of Cetane Index for Alternative Compression Ignition Engine Fuels. *Fuel* **2010**, *89*, 3807-3813.
- (3) Gregg, S. D.; Campbell, J. L.; Fisher, J. W.; Bartlett, M. G. Methods for the Characterization of Jet Propellant-8: Vapor and Aerosol. *Biomed. Chromatogr.* **2007**, *21*, 463-472.
- (4) Gough, R. V.; Bruno, T. J. Composition-Explicit Distillation Curves of Alternative Turbine Fuels. *Energy Fuels* **2013**, *27*, 294-302.
- (5) Meylemans, H. A.; Baldwin, L. C.; Harvey, B. G. Low-Temperature Properties of Renewable High-Density Fuel Blends. *Energy Fuels* **2013**, *27*, 883-888.
- (6) Witten, M., L.; Zeiger, E.; Ritchie, G. D., *Jet Fuel Toxicology*. CRC Press: 2011.
- (7) Rodgers, R. P.; Blumer, E. N.; Freitas, M. A.; Marshall, A. G. Jet Fuel Chemical Composition, Weathering, and Identification as a Contaminant at a Remediation Site, Determined by Fourier Transform Ion Cyclotron Resonance Mass Spectrometry. *Anal. Chem.* **1999**, *71*, 5171-5176.
- (8) DuBois, T. G.; Nieh, S. In *Effects of Hydrocarbon Chemical Class Composition on Autothermal Reforming of JP-8 Fuel*, Power Sources Conference, Las Vegas, Nevada, USA, Jun. 14-17;
- (9) Echavarria, C. A.; Jaramillo, I. C.; Sarofim, A. F.; Lighty, J. S. Burnout of Soot Particles in a Two-Stage Burner With a JP-8 Surrogate Fuel. *Combust. Flame* **2012**, *159*, 2441-2448.
- (10) Wang, H.; Oehlschlaeger, M. A. Autoignition Studies of Conventional and Fischer-Tropsch Jet Fuels. *Fuel* **2012**, *98*, 249-258.
- (11) Merrill, E. A.; Gearhart, J. M.; Sterner, T. R.; Robinson, P. J. Improved Predictive Model for *n*-Decane Kinetics Across Species, as a Component of Hydrocarbon Mixtures. *Inhal. Toxicol.* **2008**, *20*, 851-63.
- (12) Holley, A. T.; Dong, Y.; Andac, M. G.; Egolfopoulos, F. N.; Edwards, T. Ignition and Extinction of Non-Premixed Flames of Single-Component Liquid Hydrocarbons, Jet Fuels, and Their Surrogates. *Proc. Combust. Inst.* **2007**, *31*, 1205-1213.
- (13) Pitz, W. J.; Cernansky, N. P.; Dryer, F. L.; Egolfopoulos, F. N.; Farrell, J. T.; Friend, D. G.; Pitsch, H., Development of an Experimental Database and Chemical Kinetic Models for Surrogate Gasoline Fuels. SAE International: 2007.
- (14) Allen, C.; Valco, D.; Toulson, E.; Edwards, T.; Lee, T. Ignition Behavior and Surrogate Modeling of Jp-8 and of Camelina and Tallow Hydrotreated Renewable Jet Fuels at Low Temperatures. *Combust. Flame* **2013**, *160*, 232-239.
- (15) Natelson, R. H.; Kurman, M. S.; Johnson, R. O.; Cernansky, N. P.; Miller, D. L. Preignition and Autoignition Chemistry of the Xylene Isomers. *Combust. Sci. Technol.* **2011**, *183*, 897-914.
- (16) Joklik, R.; Fuller, C.; Turner, B.; Gokulakrishnan, P. In *The Effect of Multi-Component Fuel Evaporation on the Ignition of JP-8*, ASME Turbo Expo 2010: Power for Land, Sea, and Air, Glasgow, UK,
- (17) Honnet, S.; Seshadri, K.; Niemann, U.; Peters, N. A Surrogate Fuel for Kerosene. *Proc. Combust. Inst.* **2009**, *32*, 485-492.
- (18) Tosatto, L.; Mantia, B. L.; Bufferand, H.; Duchaine, P.; Gomez, A. Chemical Structure of a Methane Counterflow Diffusion Flame Perturbed with the Addition of either JP-8 or a Jet Fuel Surrogate. *Proc. Combust. Inst.* **2009**, *32*, 1319-1326.
- (19) Lenhert, D. B.; Miller, D. L.; Cernansky, N. P. The Oxidation of JP-8, Jet-A, and Their Surrogates in the Low and Intermediate Temperature Regime at Elevated Pressures. *Combust. Sci. Technol.* **2007**, *179*, 845-861.
- (20) Kahandawala, M. S. P.; DeWitt, M. J.; Corporan, E.; Sidhu, S. S. Ignition and Emission Characteristics of Surrogate and Practical Jet Fuels. *Energy Fuels* **2008**, *22*, 3673-3679.
- (21) Katta, V. R.; Roquemore, W. M. In *Performance of JP-8 Surrogates and Parent Species in a Swirl Combustor*, ASME Turbo Expo 2010: Power for Land, Sea, and Air, Glasgow, UK,

- (22) Ji, C.; Sarathy, S. M.; Veloo, P. S.; Westbrook, C. K.; Egolfopoulos, F. N. Effects of Fuel Branching on the Propagation of Octane Isomers Flames. *Combust. Flame* **2012**, *159*, 1426-1436.
- (23) Natelson, R. H.; Johnson, R. O.; Kurman, M. S.; Cernansky, N. P.; Miller, D. L. Comparison of Reactivity in a Flow Reactor and a Single Cylinder Engine. *Exp. Therm Fluid Sci.* **2010**, *34*, 928-932.
- (24) Caton, P. A.; Hamilton, L. J.; Cowart, J. S. Understanding Ignition Delay Effects With Pure Component Fuels in a Single-Cylinder Diesel Engine. *J. Eng. Gas. Turb. Power* **2011**, *133*, 032803.
- (25) Tosatto, L.; Mella, F.; Long, M. B.; Smooke, M. D. A Study of JP-8 Surrogate Coflow Flame Structure by Combined Use of Laser Diagnostics and Numerical Simulation. *Combust. Flame* **2012**, *159*, 3027-3039.
- (26) Mawid, M. A.; Park, T. W.; Sekar, B.; Arana, C. In *Development and Validation of A Detailed JP-8 Fuel Chemistry Model*, 2nd JANNAF Modeling and Simulation Subcommittee Meeting, Destin, Florida,
- (27) Miller, J. A.; Pilling, M. J.; Troe, J. Unravelling Combustion Mechanisms Through a Quantitative Understanding of Elementary Reactions. *Proc. Combust. Inst.* **2005**, *30*, 43-88.
- (28) Violi, A.; Yan, S.; Eddings, E. G.; Sarofim, F.; Granata, S.; Faravelli, T.; Ranzi, E. Experimental Formulation and Kinetic Model for JP-8 Surrogate Mixtures. *Combust. Sci. Technol.* **2002**, *174*, 399-417.
- (29) Podlesak, T.; Hendrickson, M.; Matthews, S.; Nawrocki, E.; Seibert, M.; Zalewski, M. Army Stirling Engine Research and Development - Past, Present and Future. *Power Sources Conference* **2010**, *44*, 462-465.
- (30) Malewicki, T.; Brezinsky, K. Experimental and Modeling Study on the Pyrolysis and Oxidation of *n*-Decane and *n*-Dodecane. *Proc. Combust. Inst.* **2013**, *34*, 361-368.
- (31) MacDonald, M. E.; Ren, W.; Zhu, Y.; Davidson, D. F.; Hanson, R. K. Fuel and Ethylene Measurements During *n*-Dodecane, Methylcyclohexane, and *iso*-Cetane Pyrolysis in Shock Tubes. *Fuel* **2013**, *103*, 1060-1068.
- (32) Banerjee, S.; Tangko, R.; Sheen, D. A.; Wang, H.; Bowman, C. T. An Experimental and Kinetic Modeling Study of *n*-Dodecane Pyrolysis and Oxidation. *Combust. Flame* **2016**, *163*, 12-30.
- (33) Dahm, K. D.; Virk, P. S.; Bounaceur, R.; Battin-Leclerc, F.; Marquaire, P. M.; Fournet, R.; Daniau, E.; Bouchez, M. Experimental and Modelling Investigation of the Thermal Decomposition of *n*-Dodecane. *J. Anal. Appl. Pyrolysis* **2004**, *71*, 865-881.
- (34) Herbinet, O.; Marquaire, P. M.; Battin-Leclerc, F.; Fournet, R. Thermal Decomposition of *n*-Dodecane: Experiments and Kinetic Modeling. *J. Anal. Appl. Pyrolysis* **2007**, *78*, 419-429.
- (35) Zhou, P. H.; Hollis, O. L.; Crynes, B. L. Thermolysis of Higher Molecular-Weight Straight-Chain Alkanes C9-C22. *Ind. Eng. Chem. Res.* **1987**, *26*, 846-852.
- (36) Yu, J.; Eser, S. Thermal Decomposition of C10-C14 Normal Alkanes in Near-Critical and Supercritical Regions: Product Distributions and Reaction Mechanisms. *Ind. Eng. Chem. Res.* **1997**, *36*, 574-584.
- (37) Yu, J.; Eser, S. Kinetics of Supercritical-Phase Thermal Decomposition of C10-C14 Normal Alkanes and Their Mixtures. *Ind. Eng. Chem. Res.* **1997**, *36*, 585-591.
- (38) Ranzi, E.; Frassoldati, A.; Granata, S.; Faravelli, T. Wide-Range Kinetic Modeling Study of the Pyrolysis, Partial Oxidation, and Combustion of Heavy *n*-Alkanes. *Ind. Eng. Chem. Res.* **2005**, *44*, 5170-5183.
- (39) Stagni, A.; Cuoci, A.; Frassoldati, A.; Faravelli, T.; Ranzi, E. Lumping and Reduction of Detailed Kinetic Schemes: an Effective Coupling. *Ind. Eng. Chem. Res.* **2014**, *53*, 9004-9016.
- (40) Biet, J.; Hakka, M. H.; Warth, V.; Glaude, P. A.; Battin-Leclerc, F. Experimental and Modeling Study of the Low-Temperature Oxidation of Large Alkanes. *Energy Fuels* **2008**, *22*, 2258-2269.
- (41) You, X. Q.; Egolfopoulos, F. N.; Wang, H. Detailed and Simplified Kinetic Models of *n*-Dodecane Oxidation: The Role of Fuel Cracking in Aliphatic Hydrocarbon Combustion. *Proc. Combust. Inst.* **2009**, *32*, 403-410.
- (42) Dooley, S.; Won, S. H.; Chaos, M.; Heyne, J.; Ju, Y.; Dryer, F. L.; Kumar, K.; Sung, C.-J.; Wang, H.; Oehlschlaeger, M. A. et al. A Jet Fuel Surrogate Formulated by Real Fuel Properties. *Combust. Flame* **2010**, *157*, 2333-2339.

- (43) Westbrook, C. K.; Pitz, W. J.; Herbinet, O.; Curran, H. J.; Silke, E. J. A Comprehensive Detailed Chemical Kinetic Reaction Mechanism for Combustion of *n*-Alkane Hydrocarbons from *n*-Octane to *n*-Hexadecane. *Combust. Flame* **2009**, *156*, 181-199.
- (44) Narayanaswamy, K.; Pepiot, P.; Pitsch, H. A Chemical Mechanism for Low to High Temperature Oxidation of *n*-Dodecane as a Component of Transportation Fuel Surrogates. *Combust. Flame* **2014**, *161*, 866-884.
- (45) Zhao, L.; Yang, T.; Kaiser, R. I.; Troy, T. P.; Ahmed, M.; Belisario-Lara, D.; Ribeiro, J. M.; Mebel, A. M. A Combined Experimental and Computational Study on the Unimolecular Decomposition of JP-8 Jet Fuel Surrogates I: *n*-Decane (*n*-C₁₀H₂₂). Submitted.
- (46) Cool, T. A.; McIlroy, A.; Qi, F.; Westmoreland, P. R.; Poisson, L.; Peterka, D. S.; Ahmed, M. Photoionization Mass Spectrometer for Studies of Flame Chemistry With a Synchrotron Light Source. *Rev. Sci. Instrum.* **2005**, *76*, 094102.
- (47) Qi, F.; Yang, R.; Yang, B.; Huang, C. Q.; Wei, L. X.; Wang, J.; Sheng, L. S.; Zhang, Y. W. Isomeric Identification of Polycyclic Aromatic Hydrocarbons Formed in Combustion With Tunable Vacuum Ultraviolet Photoionization. *Rev. Sci. Instrum.* **2006**, *77*, 084101.
- (48) Yang, B.; Li, Y. Y.; Wei, L. X.; Huang, C. Q.; Wang, J.; Tian, Z. Y.; Yang, R.; Sheng, L. S.; Zhang, Y. W.; Qi, F. An Experimental Study of the Premixed Benzene/Oxygen/Argon Flame With Tunable Synchrotron Photoionization. *Proc. Combust. Inst.* **2007**, *31*, 555-563.
- (49) Yang, B.; Oßwald, P.; Li, Y.; Wang, J.; Wei, L.; Tian, Z.; Qi, F.; Kohse-Höinghaus, K. Identification of Combustion Intermediates in Isomeric Fuel-Rich Premixed Butanol–Oxygen Flames at Low Pressure. *Combust. Flame* **2007**, *148*, 198-209.
- (50) Li, Y. Y.; Zhang, L. D.; Tian, Z. Y.; Yuan, T.; Wang, J.; Yang, B.; Qi, F. Experimental Study of a Fuel-Rich Premixed Toluene Flame at Low Pressure. *Energy Fuels* **2009**, *23*, 1473-1485.
- (51) Li, Y. Y.; Zhang, L. D.; Tian, Z. Y.; Yuan, T.; Zhang, K. W.; Yang, B.; Qi, F. Investigation of the Rich Premixed Laminar Acetylene/Oxygen/Argon Flame: Comprehensive Flame Structure and Special Concerns of Polyynes. *Proc. Combust. Inst.* **2009**, *32*, 1293-1300.
- (52) Li, Y. Y.; Qi, F. Recent Applications of Synchrotron VUV Photoionization Mass Spectrometry: Insight into Combustion Chemistry. *Acc. Chem. Res.* **2010**, *43*, 68-78.
- (53) Zhang, L. D.; Cai, J. H.; Zhang, T. C.; Qi, F. Kinetic Modeling Study of Toluene Pyrolysis at Low Pressure. *Combust. Flame* **2010**, *157*, 1686-1697.
- (54) Oßwald, P.; Güldenberg, H.; Kohse-Höinghaus, K.; Yang, B.; Yuan, T.; Qi, F. Combustion of Butanol Isomers – A Detailed Molecular Beam Mass Spectrometry Investigation of Their Flame Chemistry. *Combust. Flame* **2011**, *158*, 2-15.
- (55) Qi, F. Combustion Chemistry Probed by Synchrotron VUV Photoionization Mass Spectrometry. *Proc. Combust. Inst.* **2013**, *34*, 33-63.
- (56) Cool, T. A.; Nakajima, K.; Taatjes, C. A.; McIlroy, A.; Westmoreland, P. R.; Law, M. E.; Morel, A. Studies of a Fuel-Rich Propane Flame With Photoionization Mass Spectrometry. *Proc. Combust. Inst.* **2005**, *30*, 1681-1688.
- (57) Cool, T. A.; Wang, J.; Nakajima, K.; Taatjes, C. A.; McIlroy, A. Photoionization Cross Sections for Reaction Intermediates in Hydrocarbon Combustion. *Int. J. Mass spectrom.* **2005**, *247*, 18-27.
- (58) Zhang, F. T.; Kaiser, R. I.; Kislov, V. V.; Mebel, A. M.; Golan, A.; Ahmed, M. A VUV Photoionization Study of the Formation of the Indene Molecule and Its Isomers. *J. Phys. Chem. Lett.* **2011**, *2*, 1731-1735.
- (59) Kaiser, R. I.; Belau, L.; Leone, S. R.; Ahmed, M.; Wang, Y. M.; Braams, B. J.; Bowman, J. M. A Combined Experimental and Computational Study on the Ionization Energies of the Cyclic and Linear C₃H Isomers. *ChemPhysChem* **2007**, *8*, 1236-1239.
- (60) Kaiser, R. I.; Maksyutenko, P.; Ennis, C.; Zhang, F. T.; Gu, X. B.; Krishtal, S. P.; Mebel, A. M.; Kostko, O.; Ahmed, M. Untangling the Chemical Evolution of Titan's Atmosphere and Surface-from Homogeneous to Heterogeneous Chemistry. *Faraday Discuss.* **2010**, *147*, 429-478.
- (61) Kaiser, R. I.; Mebel, A.; Kostko, O.; Ahmed, M. On the Ionization Energies of C₄H₃ Isomers. *Chem. Phys. Lett.* **2010**, *485*, 281-285.

- (62) Kaiser, R. I.; Sun, B. J.; Lin, H. M.; Chang, A. H. H.; Mebel, A. M.; Kostko, O.; Ahmed, M. An Experimental and Theoretical Study on the Ionization Energies of Polyynes ($\text{H}-(\text{C}\equiv\text{C})_n\text{-H}$; $n=1-9$). *Astrophys. J.* **2010**, *719*, 1884-1889.
- (63) Kostko, O.; Zhou, J.; Sun, B. J.; Shiuian Lie, J.; Chang, A. H. H.; Kaiser, R. I.; Ahmed, M. Determination of Ionization Energies of C_nN ($n=4-12$): Vacuum Ultraviolet Photoionization Experiments and Theoretical Calculations. *Astrophys. J.* **2010**, *717*, 674-682.
- (64) Kaiser, R. I.; Krishtal, S. P.; Mebel, A. M.; Kostko, O.; Ahmed, M. An Experimental and Theoretical Study of the Ionization Energies of SiC_2H_x ($x=0, 1, 2$) Isomers. *Astrophys. J.* **2012**, *761*, 178-184.
- (65) Zhang, F. T.; Kaiser, R. I.; Golan, A.; Ahmed, M.; Hansen, N. A VUV Photoionization Study of the Combustion-Relevant Reaction of the Phenyl Radical (C_6H_5) With Propylene (C_3H_6) in a High Temperature Chemical Reactor. *J. Phys. Chem. A* **2012**, *116*, 3541-3546.
- (66) Golan, A.; Ahmed, M.; Mebel, A. M.; Kaiser, R. I. A VUV Photoionization Study of The Multichannel Reaction of Phenyl Radicals With 1,3-Butadiene Under Combustion Relevant Conditions. *Phys. Chem. Chem. Phys.* **2013**, *15*, 341-347.
- (67) Parker, D. S.; Kaiser, R. I.; Troy, T. P.; Ahmed, M. Hydrogen Abstraction/Acetylene Addition Revealed. *Angew. Chem. Int. Ed. Engl.* **2014**, *53*, 7740-7744.
- (68) Urness, K. N.; Guan, Q.; Golan, A.; Daily, J. W.; Nimlos, M. R.; Stanton, J. F.; Ahmed, M.; Ellison, G. B. Pyrolysis of Furan in a Microreactor. *J. Chem. Phys.* **2013**, *139*, 124305.
- (69) Guan, Q.; Urness, K. N.; Ormond, T. K.; David, D. E.; Ellison, G. B.; Daily, J. W. The Properties of a Micro-Reactor for the Study of the Unimolecular Decomposition of Large Molecules. *Int. Rev. Phys. Chem.* **2014**, *33*, 447-487.
- (70) Photoionization Cross Section Database (Version 1.0). <http://flame.nslr.ustc.edu.cn/database/>. National Synchrotron Radiation Laboratory, Hefei, China. (2011).
- (71) Curtiss, L. A.; Raghavachari, K.; Redfern, P. C.; Rassolov, V.; Pople, J. A. Gaussian-3 (G3) Theory for Molecules Containing First and Second-Row Atoms. *J. Chem. Phys.* **1998**, *109*, 7764-7776.
- (72) Baboul, A. G.; Curtiss, L. A.; Redfern, P. C.; Raghavachari, K. Gaussian-3 Theory Using Density Functional Geometries and Zero-Point Energies. *J. Chem. Phys.* **1999**, *110*, 7650-7657.
- (73) Curtiss, L. A.; Raghavachari, K.; Redfern, P. C.; Baboul, A. G.; Pople, J. A. Gaussian-3 Theory Using Coupled Cluster Energies. *Chem. Phys. Lett.* **1999**, *314*, 101-107.
- (74) Frisch, M. J.; Trucks, G. W.; Schlegel, H. B.; Scuseria, G. E.; Robb, M. A.; Cheeseman, J. R.; Scalmani, G.; Barone, V.; Mennucci, B.; Petersson, G. A. et al. *Gaussian 09, Revision A.1 Gaussian Inc., Wallingford CT 2009*.
- (75) Werner, H. J.; Knowles, P. J.; Knizia, G.; Manby, F. R.; Schütz, M.; Celani, P.; Györffy, W.; Kats, D.; Korona, T.; Lindh, R. et al., MOLPRO, version 2010.1, a package of ab initio programs, <http://www.molpro.net>.
- (76) Georgievskii, Y.; Miller, J. A.; Burke, M. P.; Klippenstein, S. J. Reformulation and Solution of the Master Equation for Multiple-Well Chemical Reactions. *J. Phys. Chem. A* **2013**, *117*, 12146-12154.
- (77) Georgievskii, Y.; Klippenstein, S. J., MESS.2016.3.23, <http://tcg.cse.anl.gov/papr/codes/mess.html>.
- (78) Troe, J. Theory of Thermal Unimolecular Reactions at Low Pressures. I. Solutions of the Master Equation. *J. Chem. Phys.* **1977**, *66*, 4745-4757.
- (79) Jasper, A. W.; Oana, C. M.; Miller, J. A. "Third-Body" Collision Efficiencies for Combustion Modeling: Hydrocarbons in Atomic and Aiatomic Baths. *Proc. Combust. Inst.* **2015**, *35*, 197-204.
- (80) Jasper, A. W.; Miller, J. A. Lennard-Jones Parameters for Combustion and Chemical Kinetics Modeling from Full-Dimensional Intermolecular Potentials. *Combust. Flame* **2014**, *161*, 101-110.
- (81) Harding, L. B.; Georgievskii, Y.; Klippenstein, S. J. Predictive Theory for Hydrogen Atom - Hydrocarbon Radical Association Kinetics. *J. Phys. Chem. A* **2005**, *109*, 4646-4656.
- (82) Klippenstein, S. J.; Georgievskii, Y.; Harding, L. B. Predictive Theory for the Combination Kinetics of Two Alkyl Radicals. *Phys. Chem. Chem. Phys.* **2006**, *8*, 1133-1147.
- (83) Active Thermochemical Tables, <http://atct.anl.gov/Thermochemical%20Data/version%201.118/index.php>.

- (84) Sivaramakrishnan, R.; Michael, J. V.; Ruscic, B. High-Temperature Rate Constants for H/D + C₂H₆ and C₃H₈. *Int. J. Chem. Kinet.* **2012**, *44*, 194-205.
- (85) Tsang, W. Chemical Kinetic Data-Base for Combustion Chemistry. Part 3. Propane. *J. Phys. Chem. Ref. Data* **1988**, *17*, 887-952.
- (86) Baldwin, R. R.; Walker, R. W. Rate Constants for Hydrogen + Oxygen System, and for H Atoms and OH Radicals + Alkanes. *J. Chem. Soc. Faraday Trans.* **1979**, *75*, 140-154.
- (87) Stewart, J.; Brezinsky, K.; Glassman, I. Supercritical Pyrolysis of Decalin, Tetralin, and *n*-Decane at 700-800K. Product Distribution and Reaction Mechanism. *Combust. Sci. Technol.* **1998**, *136*, 373-390.
- (88) Glassman, I.; Yetter, R. A.; Glumac, N. G., *Combustion*. Academic press: 2014.
- (89) Chang, A. H. H.; Mebel, A. M.; Yang, X. M.; Lin, S. H.; Lee, Y. T. Ab Initio/RRKM Approach toward the Understanding of Ethylene Photodissociation. *J. Chem. Phys.* **1998**, *109*, 2748-2761.
- (90) Narendrapurapu, B. S.; Simmonett, A. C.; Schaefer-III, H. F.; Miller, J. A.; Klippenstein, S. J. Combustion Chemistry: Important Features of the C₃H₅ Potential Energy Surface, Including Allyl Radical, Propargyl + H₂, Allene + H, and Eight Transition States. *J. Phys. Chem. A* **2011**, *115*, 14209-14214.
- (91) Hansen, N.; Miller, J. A.; Westmoreland, P. R.; Kasper, T.; Kohse-Höinghaus, K.; Wang, J.; Cool, T. A. Isomer-Specific Combustion Chemistry in Allene and Propyne Flames. *Combust. Flame* **2009**, *156*, 2153-2164.
- (92) Miller, J. A.; Senosiain, J. P.; Klippenstein, S. J.; Georgievskii, Y. Reactions over Multiple, Interconnected Potential Wells: Unimolecular and Bimolecular Reactions on a C₃H₅ Potential. *J. Phys. Chem. A* **2008**, *112*, 9429-9438.
- (93) Chin, C. H.; Lee, S. H. Comparison of Two-Body and Three-Body Decomposition of Ethanedial, Propanal, Propenal, *n*-Butane, 1-Butene, and 1,3-Butadiene. *J. Chem. Phys.* **2012**, *136*, 024308.
- (94) Ribeiro, J. M.; Mebel, A. M. Reaction Mechanism and Product Branching Ratios of the CH + C₃H₆ Reaction: A Theoretical Study. *J. Phys. Chem. A* **2016**, *120*, 1800-1812.
- (95) Backx, C.; Wight, G. R.; Wiel, M. J. V. d. Oscillator Strengths (10-70 eV) for Absorption, Ionization and Dissociation in H₂, HD and D₂, Obtained by an Electron-Ion Coincidence Method. *J. Phys. B: At. Mol. Opt. Phys.* **1976**, *9*, 315.
- (96) Savee, J. D.; Soorkia, S.; Welz, O.; Selby, T. M.; Taatjes, C. A.; Osborn, D. L. Absolute Photoionization Cross-Section of the Propargyl Radical. *J. Chem. Phys.* **2012**, *136*, 134307.
- (97) Samson, J. A. R.; Haddad, G. N.; Masuoka, T.; Pareek, P. N.; Kilcoyne, D. A. L. Ionization Yields, Total Absorption, and Dissociative Photoionization Cross-Sections of CH₄ from 110-950-Å. *J. Chem. Phys.* **1989**, *90*, 6925-6932.
- (98) Gans, B.; Garcia, G. A.; Boyé-Péronne, S.; Loison, J.-C.; Douin, S.; Gaie-Levrel, F.; Gauyacq, D. Absolute Photoionization Cross Section of the Ethyl Radical in the Range 8–11.5 eV: Synchrotron and Vacuum Ultraviolet Laser Measurements. *J. Phys. Chem. A* **2011**, *115*, 5387-5396.
- (99) Yang, B.; Wang, J.; Cool, T. A.; Hansen, N.; Skeen, S.; Osborn, D. L. Absolute Photoionization Cross-Sections of Some Combustion Intermediates. *Int. J. Mass spectrom.* **2012**, *309*, 118-128.
- (100) Robinson, J. C.; Sveum, N. E.; Neumark, D. M. Determination of Absolute Photoionization Cross Sections for Isomers of C₃H₅: Allyl and 2-Propenyl Radicals. *Chem. Phys. Lett.* **2004**, *383*, 601-605.
- (101) Koizumi, H. Predominant Decay Channel for Superexcited Organic-Molecules. *J. Chem. Phys.* **1991**, *95*, 5846-5852.
- (102) Wang, J.; Yang, B.; Cool, T. A.; Hansen, N.; Kasper, T. Near-Threshold Absolute Photoionization Cross-Sections of Some Reaction Intermediates in Combustion. *Int. J. Mass spectrom.* **2008**, *269*, 210-220.
- (103) Zhou, Z. Y.; Zhang, L. D.; Xie, M. F.; Wang, Z. D.; Chen, D. N.; Qi, F. Determination of Absolute Photoionization Cross-Sections of Alkanes and Cyclo-Alkanes. *Rapid Commun. Mass Spectrom.* **2010**, *24*, 1335-1342.



TOC graphic

Supporting Information

A Combined Experimental and Computational Study on the Unimolecular Decomposition of JP-8 Jet Fuel Surrogates II: *n*-Dodecane (*n*-C₁₂H₂₆)

Long Zhao, Tao Yang, Ralf I. Kaiser*

Department of Chemistry, University of Hawaii at Manoa, Honolulu, Hawaii, 96822

Tyler P. Troy, Musahid Ahmed*

*Chemical Sciences Division, Lawrence Berkeley National Laboratory, Berkeley, California
94720*

Joao Marcelo Ribeiro, Daniel Belisario-Lara, Alexander M. Mebel*

*Department of Chemistry and Biochemistry, Florida International University, Miami, Florida
33199*

Table S1. Detected molecules in previous experimental studies of *n*-dodecane pyrolysis.

Molecule	Formula	Mass	Structure	Ref.
Hydrogen	H ₂	2	H—H	1
Methane	CH ₄	16	CH ₄	1-5
Acetylene	C ₂ H ₂	26		1-3
Ethylene	C ₂ H ₄	28		1-8
Ethane	C ₂ H ₆	30		1-5
Allene	C ₃ H ₄	40		1,3
Methylacetylene	C ₃ H ₄	40		1,3
Propene	C ₃ H ₆	42		1-5,7-8
Propane	C ₃ H ₈	44		5,7-8
Diacetylene	C ₄ H ₂	50		3
Vinylacetylene	C ₄ H ₄	52		3
1,3-Butadiene	C ₄ H ₆	54		1-3
1-Butene	C ₄ H ₈	56		1-5,7-8
2-Butene	C ₄ H ₈	56		5,7-8
Cyclopentadiene	C ₅ H ₆	66		1
Cyclopentene	C ₅ H ₈	68		1
1-Pentene	C ₅ H ₁₀	70		1-4,7-8
2-Pentene	C ₅ H ₁₀	70		5,7-8
<i>n</i> -Pentane	C ₅ H ₁₂	72		5,7-8
Benzene	C ₆ H ₆	78		1,3
1,3-Hexadiene	C ₆ H ₁₀	82		2
1-Hexene	C ₆ H ₁₂	84		1-5,7-8
2-Hexene	C ₆ H ₁₂	84		5,7-8
<i>n</i> -Hexane	C ₆ H ₁₄	86		7-8
Toluene	C ₇ H ₈	92		1
1-Heptene	C ₇ H ₁₄	98		1-4,7-8
2-Heptene	C ₇ H ₁₄	98		5,7-8
<i>n</i> -Heptane	C ₇ H ₁₆	100		7-8

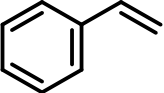
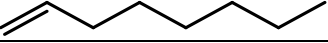
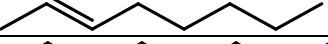
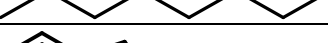
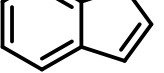
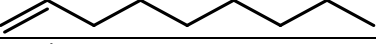
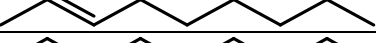

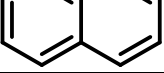
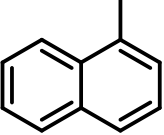
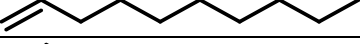
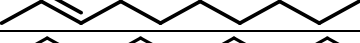
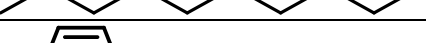
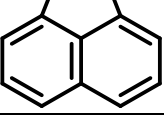
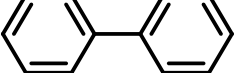
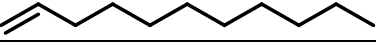


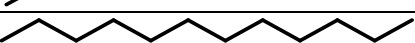
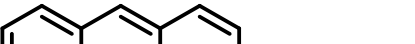

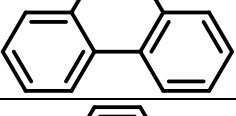
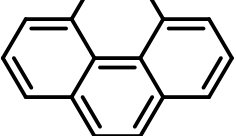
Styrene	C_8H_8	104		1
1-Octene	C_8H_{16}	112		1-3,5,7-8
2-Octene	C_8H_{16}	112		7-8
<i>n</i> -Octane	C_8H_{18}	114		5,7-8
Indene	C_9H_8	116		1
1-Nonene	C_9H_{18}	126		1-3,5,7-8
2-Nonene	C_9H_{18}	126		7-8
<i>n</i> -Nonane	C_9H_{20}	128		5,7-8
Naphthalene	$C_{10}H_8$	128		1
Methylnaphthalene	$C_{11}H_{10}$	142		1
1-Decene	$C_{10}H_{20}$	140		1-3,5,7-8
1-Decene	$C_{10}H_{20}$	140		7-8
<i>n</i> -Decane	$C_{10}H_{22}$	142		5,7-8
Acenaphthalene	$C_{12}H_8$	152		1
Biphenyl	$C_{12}H_{10}$	154		1
1-Undecene	$C_{11}H_{22}$	154		1,3,5,7-8
1-Undecene	$C_{11}H_{22}$	154		7-8
<i>n</i> -Undecane	$C_{11}H_{24}$	156		5,7-8
1-Dodecene	$C_{12}H_{24}$	168		5,7-8
<i>n</i> -Dodecane	$C_{12}H_{26}$	170		1-8
Anthracene	$C_{14}H_{10}$	178		1
Phenathrene	$C_{14}H_{10}$	178		1
Pyrene	$C_{16}H_{10}$	202		1

Table S2. Parameters of the fitted modified Arrhenius expressions, $A \cdot T^\alpha \cdot \exp(-E_a/RT)$, for most important reactions involved in pyrolysis of *n*-dodecane at pressures of 0.03-0.04, 1, 10, and 100 atm.

The data are presented in the following order:

$/p, \text{atm}$ $A, \text{cm}^3 \text{mol}^{-1} \text{s}^{-1}$ α $E_a, \text{cal mol}^{-1}/$! fit btw. T_1 and T_2 with MAE = mean/max absolute error
 The title line for each reaction shows A , α , and E_a at the high-pressure limit.
 The fits are provided to a single Arrhenius expression and to a sum of two Arrhenius expressions

C₁₂H₂₆ → C₂H₅ + C₁₀H₂₁			3.81E+67	-14.27	110300.0	
PLOG/3.000E-02	2.27E+107	-26.56	125300.0/			! fit btw. 500 and 2500 K with MAE of 44.6%, 153.4%
PLOG/3.947E-02	2.64E+106	-26.26	125100.0/			! fit btw. 500 and 2500 K with MAE of 44.5%, 155.5%
PLOG/1.000E+00	8.94E+92	-22.00	120800.0/			! fit btw. 500 and 2500 K with MAE of 49.3%, 165.1%
PLOG/1.000E+01	8.35E+80	-18.31	116100.0/			! fit btw. 500 and 2500 K with MAE of 53.7%, 157.2%
PLOG/1.000E+02	3.81E+67	-14.27	110300.0/			! fit btw. 500 and 2500 K with MAE of 53.0%, 124.8%
PLOG/3.000E-02	7.61E+253	-74.12	166000.0/			
PLOG/3.000E-02	2.28E+122	-30.73	136700.0/			! fit btw. 500 and 2500 K with MAE of 29.5%, 63.2%
PLOG/3.947E-02	2.00E+122	-30.67	137200.0/			
PLOG/3.947E-02	8.60E+256	-75.03	167400.0/			! fit btw. 500 and 2500 K with MAE of 28.3%, 60.4%
PLOG/1.000E+00	-2.37E+98	-23.91	118200.0/			
PLOG/1.000E+00	8.43E+86	-20.36	113800.0/			! fit btw. 500 and 2500 K with MAE of 38.0%, 63.1%
PLOG/1.000E+01	3.25E+109	-26.20	139000.0/			
PLOG/1.000E+01	1.22E+102	-25.86	116800.0/			! fit btw. 500 and 2500 K with MAE of 16.8%, 35.8%
PLOG/1.000E+02	2.48E+57	-11.63	102500.0/			
PLOG/1.000E+02	8.17E+142	-35.04	172800.0/			! fit btw. 500 and 2500 K with MAE of 8.1%, 20.9%
C₁₂H₂₆ → C₃H₇ + C₉H₁₉			3.14E+68	-14.45	111400.0	
PLOG/3.000E-02	3.92E+108	-26.85	126500.0/			! fit btw. 500 and 2500 K with MAE of 45.0%, 154.5%
PLOG/3.947E-02	4.54E+107	-26.54	126300.0/			! fit btw. 500 and 2500 K with MAE of 44.9%, 156.7%
PLOG/1.000E+00	1.28E+94	-22.26	122000.0/			! fit btw. 500 and 2500 K with MAE of 49.6%, 166.8%
PLOG/1.000E+01	9.40E+81	-18.53	117200.0/			! fit btw. 500 and 2500 K with MAE of 54.1%, 159.5%
PLOG/1.000E+02	3.14E+68	-14.45	111400.0/			! fit btw. 500 and 2500 K with MAE of 53.5%, 126.8%
PLOG/3.000E-02	5.15E+254	-74.29	167000.0/			
PLOG/3.000E-02	3.09E+123	-30.98	137800.0/			! fit btw. 500 and 2500 K with MAE of 29.9%, 64.4%
PLOG/3.947E-02	2.84E+123	-30.93	138300.0/			
PLOG/3.947E-02	6.69E+255	-74.59	167700.0/			! fit btw. 500 and 2500 K with MAE of 28.7%, 61.5%

PLOG/1.000E+00	-4.90E+99	-24.21	119700.0/	
PLOG/1.000E+00	1.91E+88	-20.67	115300.0/	! fit btw. 500 and 2500 K with MAE of 37.8%, 62.1%
PLOG/1.000E+01	6.68E+110	-26.49	140400.0/	
PLOG/1.000E+01	2.36E+102	-25.85	117600.0/	! fit btw. 500 and 2500 K with MAE of 16.9%, 35.9%
PLOG/1.000E+02	1.31E+58	-11.75	103500.0/	
PLOG/1.000E+02	1.77E+144	-35.34	174200.0/	! fit btw. 500 and 2500 K with MAE of 8.2%, 20.9%

C₁₂H₂₆ → C₄H₉ + C₈H₁₇

1.96E+68 -14.42 111300.0

PLOG/3.000E-02	2.18E+108	-26.80	126300.0/	! fit btw. 500 and 2500 K with MAE of 45.0%, 154.4%
PLOG/3.947E-02	2.53E+107	-26.50	126100.0/	! fit btw. 500 and 2500 K with MAE of 44.8%, 156.6%
PLOG/1.000E+00	7.35E+93	-22.22	121800.0/	! fit btw. 500 and 2500 K with MAE of 49.6%, 166.6%
PLOG/1.000E+01	5.59E+81	-18.49	117000.0/	! fit btw. 500 and 2500 K with MAE of 54.1%, 159.2%
PLOG/1.000E+02	1.96E+68	-14.42	111300.0/	! fit btw. 500 and 2500 K with MAE of 53.5%, 126.5%

PLOG/3.000E-02	3.58E+254	-74.27	166800.0/	
PLOG/3.000E-02	1.81E+123	-30.94	137700.0/	! fit btw. 500 and 2500 K with MAE of 29.9%, 64.2%
PLOG/3.947E-02	1.63E+123	-30.89	138100.0/	
PLOG/3.947E-02	1.15E+257	-75.01	168000.0/	! fit btw. 500 and 2500 K with MAE of 28.6%, 61.3%
PLOG/1.000E+00	-1.62E+99	-24.11	119100.0/	
PLOG/1.000E+00	8.39E+87	-20.60	114900.0/	! fit btw. 500 and 2500 K with MAE of 39.1%, 64.3%
PLOG/1.000E+01	2.35E+110	-26.39	140000.0/	
PLOG/1.000E+01	8.48E+102	-26.06	117700.0/	! fit btw. 500 and 2500 K with MAE of 16.9%, 36.1%
PLOG/1.000E+02	8.70E+57	-11.73	103300.0/	
PLOG/1.000E+02	9.51E+143	-35.29	174000.0/	! fit btw. 500 and 2500 K with MAE of 8.2%, 20.9%

C₁₂H₂₆ → C₅H₁₁ + C₇H₁₅

2.14E+68 -14.43 111300.0

PLOG/3.000E-02	2.46E+108	-26.82	126400.0/	! fit btw. 500 and 2500 K with MAE of 45.0%, 154.4%
PLOG/3.947E-02	2.85E+107	-26.52	126200.0/	! fit btw. 500 and 2500 K with MAE of 44.8%, 156.6%
PLOG/1.000E+00	8.22E+93	-22.23	121800.0/	! fit btw. 500 and 2500 K with MAE of 49.6%, 166.6%
PLOG/1.000E+01	6.19E+81	-18.51	117100.0/	! fit btw. 500 and 2500 K with MAE of 54.1%, 159.2%
PLOG/1.000E+02	2.14E+68	-14.43	111300.0/	! fit btw. 500 and 2500 K with MAE of 53.5%, 126.5%

PLOG/3.000E-02	3.81E+254	-74.28	166900.0/	
PLOG/3.000E-02	1.97E+123	-30.96	137700.0/	! fit btw. 500 and 2500 K with MAE of 29.9%, 64.3%
PLOG/3.947E-02	1.79E+123	-30.90	138200.0/	
PLOG/3.947E-02	1.32E+257	-75.03	168100.0/	! fit btw. 500 and 2500 K with MAE of 28.7%, 61.4%
PLOG/1.000E+00	-1.40E+99	-24.07	119300.0/	
PLOG/1.000E+00	1.34E+88	-20.66	115000.0/	! fit btw. 500 and 2500 K with MAE of 38.3%, 65.8%

PLOG/1.000E+01	4.25E+110	-26.46	140200.0/	
PLOG/1.000E+01	1.64E+102	-25.84	117500.0/	! fit btw. 500 and 2500 K with MAE of 16.8%, 35.9%
PLOG/1.000E+02	9.37E+57	-11.74	103400.0/	
PLOG/1.000E+02	1.09E+144	-35.31	174100.0/	! fit btw. 500 and 2500 K with MAE of 8.2%, 21.1%

C₁₂H₂₆ → C₆H₁₃ + C₆H₁₃

2.43E+68 -14.43 111300.0

PLOG/3.000E-02	2.80E+108	-26.82	126400.0/	! fit btw. 500 and 2500 K with MAE of 45.0%, 154.4%
PLOG/3.947E-02	3.25E+107	-26.51	126200.0/	! fit btw. 500 and 2500 K with MAE of 44.8%, 156.6%
PLOG/1.000E+00	9.36E+93	-22.23	121800.0/	! fit btw. 500 and 2500 K with MAE of 49.6%, 166.6%
PLOG/1.000E+01	7.04E+81	-18.50	117100.0/	! fit btw. 500 and 2500 K with MAE of 54.1%, 159.2%
PLOG/1.000E+02	2.43E+68	-14.43	111300.0/	! fit btw. 500 and 2500 K with MAE of 53.5%, 126.6%

PLOG/3.000E-02	4.12E+254	-74.27	166900.0/	
PLOG/3.000E-02	2.28E+123	-30.96	137700.0/	! fit btw. 500 and 2500 K with MAE of 29.9%, 64.2%
PLOG/3.947E-02	2.06E+123	-30.90	138200.0/	
PLOG/3.947E-02	1.42E+257	-75.02	168100.0/	! fit btw. 500 and 2500 K with MAE of 28.7%, 61.4%
PLOG/1.000E+00	-2.13E+99	-24.12	119200.0/	
PLOG/1.000E+00	9.64E+87	-20.60	114800.0/	! fit btw. 500 and 2500 K with MAE of 39.7%, 66.2%
PLOG/1.000E+01	4.86E+110	-26.46	140200.0/	
PLOG/1.000E+01	1.83E+102	-25.83	117500.0/	! fit btw. 500 and 2500 K with MAE of 16.8%, 35.9%
PLOG/1.000E+02	1.06E+58	-11.74	103400.0/	
PLOG/1.000E+02	1.23E+144	-35.30	174000.0/	! fit btw. 500 and 2500 K with MAE of 8.1%, 21.1%

C₉H₂₁ (1-nonyl) → C₂H₄ + C₇H₁₅^b

1.51E+29 -4.56 37640.0

PLOG/3.000E-02	5.15E+33	-6.79	33390.0/	! fit btw. 500 and 2500 K with MAE of 29.6%, 88.7%
PLOG/1.000E+00	1.74E+37	-7.34	38490.0/	! fit btw. 500 and 2500 K with MAE of 18.3%, 31.0%
PLOG/1.000E+01	1.11E+35	-6.45	39240.0/	! fit btw. 500 and 2500 K with MAE of 10.6%, 17.6%
PLOG/1.000E+02	1.51E+29	-4.56	37640.0/	! fit btw. 500 and 2500 K with MAE of 8.7%, 22.8%

PLOG/3.000E-02	1.61E+77	-19.82	53500.0/	
PLOG/3.000E-02	9.57E+22	-3.67	29830.0/	! fit btw. 500 and 2500 K with MAE of 3.1%, 5.7%
PLOG/1.000E+00	4.64E+48	-10.72	44080.0/	
PLOG/1.000E+00	7.47E+67	-14.95	92450.0/	! fit btw. 500 and 2500 K with MAE of 4.7%, 18.3%
PLOG/1.000E+01	8.47E+79	-19.50	66240.0/	
PLOG/1.000E+01	1.08E+26	-3.91	34190.0/	! fit btw. 500 and 2500 K with MAE of 1.4%, 3.4%
PLOG/1.000E+02	1.15E+70	-16.20	66790.0/	
PLOG/1.000E+02	1.81E+23	-2.92	33990.0/	! fit btw. 500 and 2500 K with MAE of 0.6%, 2.0%

C₁₀H₂₁ (1-decyl) → C₂H₄ + C₈H₁₇^b				7.78E+27	-4.19	37110.0
PLOG/3.000E-02	1.83E+36	-7.50	35050.0/	! fit btw. 500 and 2500 K with MAE of 33.0%, 70.9%		
PLOG/1.000E+00	1.73E+38	-7.61	39310.0/	! fit btw. 500 and 2500 K with MAE of 17.9%, 33.0%		
PLOG/1.000E+01	4.70E+34	-6.33	39280.0/	! fit btw. 500 and 2500 K with MAE of 11.0%, 18.7%		
PLOG/1.000E+02	7.78E+27	-4.19	37110.0/	! fit btw. 500 and 2500 K with MAE of 10.7%, 21.0%		
PLOG/3.000E-02	1.57E+81	-20.97	55830.0/			
PLOG/3.000E-02	9.22E+22	-3.66	29670.0/	! fit btw. 500 and 2500 K with MAE of 3.3%, 5.5%		
PLOG/1.000E+00	3.24E+47	-10.36	43780.0/			
PLOG/1.000E+00	2.71E+74	-16.63	102300.0/	! fit btw. 500 and 2500 K with MAE of 6.3%, 19.0%		
PLOG/1.000E+01	6.57E+82	-20.31	68740.0/			
PLOG/1.000E+01	3.22E+26	-4.04	34640.0/	! fit btw. 500 and 2500 K with MAE of 1.4%, 3.3%		
PLOG/1.000E+02	4.98E+67	-15.50	65840.0/			
PLOG/1.000E+02	6.14E+22	-2.79	33870.0/	! fit btw. 500 and 2500 K with MAE of 0.8%, 2.1%		
C₁₂H₂₅ (1-dodecyl) → C₂H₄ + C₁₀H₂₁^b				2.13E+28	-4.31	37400.0
PLOG/3.000E-02	6.15E+34	-7.06	34320.0/	! fit btw. 500 and 2500 K with MAE of 30.4%, 86.1%		
PLOG/3.947E-02	1.86E+35	-7.16	34830.0/	! fit btw. 500 and 2500 K with MAE of 29.6%, 79.5%		
PLOG/1.000E+00	3.62E+37	-7.41	39020.0/	! fit btw. 500 and 2500 K with MAE of 17.5%, 30.4%		
PLOG/1.000E+01	4.96E+34	-6.33	39350.0/	! fit btw. 500 and 2500 K with MAE of 10.5%, 20.5%		
PLOG/1.000E+02	2.13E+28	-4.31	37400.0/	! fit btw. 500 and 2500 K with MAE of 9.4%, 22.9%		
PLOG/3.000E-02	6.14E+81	-21.11	56370.0/			
PLOG/3.000E-02	6.46E+22	-3.60	29640.0/	! fit btw. 500 and 2500 K with MAE of 3.3%, 6.6%		
PLOG/3.947E-02	1.48E+82	-21.17	57020.0/			
PLOG/3.947E-02	7.33E+22	-3.59	29720.0/	! fit btw. 500 and 2500 K with MAE of 3.2%, 6.3%		
PLOG/1.000E+00	4.07E+47	-10.37	43950.0/			
PLOG/1.000E+00	3.27E+70	-15.59	97770.0/	! fit btw. 500 and 2500 K with MAE of 5.2%, 19.9%		
PLOG/1.000E+01	4.27E+85	-21.09	70880.0/			
PLOG/1.000E+01	3.94E+26	-4.05	34750.0/	! fit btw. 500 and 2500 K with MAE of 1.2%, 3.5%		
PLOG/1.000E+02	1.07E+67	-15.29	65680.0/			
PLOG/1.000E+02	3.93E+22	-2.73	33800.0/	! fit btw. 500 and 2500 K with MAE of 0.7%, 2.1%		
C₁₂H₂₅ (2-dodecyl) → C₃H₆ + C₉H₁₉^b				3.49E+28	-4.36	37550.0
PLOG/3.000E-02	6.83E+34	-7.07	34360.0/	! fit btw. 500 and 2500 K with MAE of 30.5%, 86.6%		
PLOG/3.947E-02	2.08E+35	-7.17	34870.0/	! fit btw. 500 and 2500 K with MAE of 29.7%, 80.0%		

PLOG/1.000E+00	4.72E+37	-7.44	39090.0/	! fit btw. 500 and 2500 K with MAE of 17.6%, 30.6%
PLOG/1.000E+01	7.40E+34	-6.38	39470.0/	! fit btw. 500 and 2500 K with MAE of 10.7%, 20.7%
PLOG/1.000E+02	3.49E+28	-4.36	37550.0/	! fit btw. 500 and 2500 K with MAE of 9.5%, 23.5%
PLOG/3.000E-02	8.43E+81	-21.15	56440.0/	
PLOG/3.000E-02	6.95E+22	-3.60	29670.0/	! fit btw. 500 and 2500 K with MAE of 3.4%, 6.5%
PLOG/3.947E-02	2.17E+82	-21.22	57100.0/	
PLOG/3.947E-02	7.98E+22	-3.59	29760.0/	! fit btw. 500 and 2500 K with MAE of 3.2%, 6.3%
PLOG/1.000E+00	7.26E+47	-10.44	44090.0/	
PLOG/1.000E+00	1.55E+70	-15.50	97230.0/	! fit btw. 500 and 2500 K with MAE of 5.3%, 20.5%
PLOG/1.000E+01	4.71E+85	-21.10	70860.0/	
PLOG/1.000E+01	4.20E+26	-4.06	34780.0/	! fit btw. 500 and 2500 K with MAE of 1.2%, 3.5%
PLOG/1.000E+02	1.92E+67	-15.36	65780.0/	
PLOG/1.000E+02	4.44E+22	-2.74	33850.0/	! fit btw. 500 and 2500 K with MAE of 0.7%, 2.1%

C₁₂H₂₅ (3-dodecyl) → C₁₁H₂₂ (1-undecene) + CH₃^b

1.46E+32 -5.40 39600.0

PLOG/3.000E-02	1.63E+34	-6.96	33710.0/	! fit btw. 500 and 2500 K with MAE of 33.4%, 108.2%
PLOG/3.947E-02	6.61E+34	-7.10	34280.0/	! fit btw. 500 and 2500 K with MAE of 32.6%, 101.5%
PLOG/1.000E+00	6.32E+38	-7.81	39450.0/	! fit btw. 500 and 2500 K with MAE of 21.9%, 36.5%
PLOG/1.000E+01	2.52E+37	-7.13	40720.0/	! fit btw. 500 and 2500 K with MAE of 12.9%, 22.5%
PLOG/1.000E+02	1.46E+32	-5.40	39600.0/	! fit btw. 500 and 2500 K with MAE of 9.6%, 26.4%
PLOG/3.000E-02	1.70E+82	-21.34	55800.0/	
PLOG/3.000E-02	3.89E+23	-3.86	30550.0/	! fit btw. 500 and 2500 K with MAE of 4.1%, 8.2%
PLOG/3.947E-02	7.54E+82	-21.48	56540.0/	
PLOG/3.947E-02	3.28E+23	-3.81	30430.0/	! fit btw. 500 and 2500 K with MAE of 3.9%, 7.2%
PLOG/1.000E+00	8.20E+53	-12.28	46770.0/	
PLOG/1.000E+00	3.39E+54	-11.50	74430.0/	! fit btw. 500 and 2500 K with MAE of 5.2%, 21.5%
PLOG/1.000E+01	4.61E+41	-8.39	42870.0/	
PLOG/1.000E+01	5.63E+140	-33.62	195800.0/	! fit btw. 500 and 2500 K with MAE of 7.0%, 24.8%
PLOG/1.000E+02	1.92E+78	-18.58	71250.0/	
PLOG/1.000E+02	9.88E+24	-3.41	35300.0/	! fit btw. 500 and 2500 K with MAE of 0.7%, 2.3%

C₁₂H₂₅ (3-dodecyl) → C₄H₈ (1-butene) + C₈H₁₇^b

5.90E+31 -5.36 38970.0

PLOG/3.000E-02	8.40E+33	-6.92	33300.0/	! fit btw. 500 and 2500 K with MAE of 32.8%, 105.5%
PLOG/3.947E-02	3.24E+34	-7.05	33860.0/	! fit btw. 500 and 2500 K with MAE of 32.1%, 99.0%
PLOG/1.000E+00	2.06E+38	-7.72	38870.0/	! fit btw. 500 and 2500 K with MAE of 21.6%, 35.8%
PLOG/1.000E+01	8.11E+36	-7.05	40080.0/	! fit btw. 500 and 2500 K with MAE of 12.6%, 22.2%

PLOG/1.000E+02	5.90E+31	-5.36	38970.0/	! fit btw. 500 and 2500 K with MAE of 9.3%, 25.3%
PLOG/3.000E-02	5.95E+80	-20.95	54840.0/	
PLOG/3.000E-02	3.07E+23	-3.87	30300.0/	! fit btw. 500 and 2500 K with MAE of 4.0%, 7.9%
PLOG/3.947E-02	2.74E+81	-21.10	55580.0/	
PLOG/3.947E-02	2.22E+23	-3.80	30120.0/	! fit btw. 500 and 2500 K with MAE of 3.7%, 7.0%
PLOG/1.000E+00	1.59E+53	-12.13	46080.0/	
PLOG/1.000E+00	1.88E+54	-11.48	74040.0/	! fit btw. 500 and 2500 K with MAE of 5.0%, 20.9%
PLOG/1.000E+01	1.39E+41	-8.30	42210.0/	
PLOG/1.000E+01	6.88E+138	-33.17	193300.0/	! fit btw. 500 and 2500 K with MAE of 6.8%, 23.9%
PLOG/1.000E+02	3.58E+78	-18.73	71040.0/	
PLOG/1.000E+02	7.97E+24	-3.44	34850.0/	! fit btw. 500 and 2500 K with MAE of 0.7%, 2.2%

C₁₂H₂₅ (4-dodecyl) → C₁₀H₂₀ (1-decene) + C₂H₅^b

1.72E+29 -4.66 37730.0

PLOG/3.000E-02	9.80E+33	-6.94	33640.0/	! fit btw. 500 and 2500 K with MAE of 31.1%, 93.0%
PLOG/3.947E-02	3.21E+34	-7.05	34170.0/	! fit btw. 500 and 2500 K with MAE of 30.4%, 86.5%
PLOG/1.000E+00	2.58E+37	-7.47	38680.0/	! fit btw. 500 and 2500 K with MAE of 19.0%, 31.9%
PLOG/1.000E+01	1.36E+35	-6.56	39370.0/	! fit btw. 500 and 2500 K with MAE of 11.2%, 18.8%
PLOG/1.000E+02	1.72E+29	-4.66	37730.0/	! fit btw. 500 and 2500 K with MAE of 9.1%, 23.9%
PLOG/3.000E-02	1.28E+81	-21.04	55550.0/	
PLOG/3.000E-02	4.28E+22	-3.64	29540.0/	! fit btw. 500 and 2500 K with MAE of 3.5%, 6.4%
PLOG/3.947E-02	4.80E+81	-21.15	56280.0/	
PLOG/3.947E-02	4.28E+22	-3.62	29550.0/	! fit btw. 500 and 2500 K with MAE of 3.3%, 6.1%
PLOG/1.000E+00	1.44E+49	-10.94	44420.0/	
PLOG/1.000E+00	6.88E+62	-13.69	86940.0/	! fit btw. 500 and 2500 K with MAE of 5.1%, 20.6%
PLOG/1.000E+01	2.13E+83	-20.56	68480.0/	
PLOG/1.000E+01	1.29E+26	-4.01	34300.0/	! fit btw. 500 and 2500 K with MAE of 1.4%, 3.7%
PLOG/1.000E+02	4.19E+71	-16.73	67940.0/	
PLOG/1.000E+02	1.27E+23	-2.96	33960.0/	! fit btw. 500 and 2500 K with MAE of 0.7%, 2.3%

C₁₂H₂₅ (4-dodecyl) → C₅H₁₀ (1-pentene) + C₇H₁₅^b

4.40E+29 -4.73 38240.0

PLOG/3.000E-02	2.05E+34	-7.00	34010.0/	! fit btw. 500 and 2500 K with MAE of 31.5%, 95.2%
PLOG/3.947E-02	6.97E+34	-7.12	34550.0/	! fit btw. 500 and 2500 K with MAE of 30.9%, 88.6%
PLOG/1.000E+00	7.37E+37	-7.56	39160.0/	! fit btw. 500 and 2500 K with MAE of 19.3%, 32.3%
PLOG/1.000E+01	3.94E+35	-6.65	39880.0/	! fit btw. 500 and 2500 K with MAE of 11.3%, 18.9%
PLOG/1.000E+02	4.40E+29	-4.73	38240.0/	! fit btw. 500 and 2500 K with MAE of 9.2%, 24.2%

PLOG/3.000E-02	3.93E+81	-21.15	55980.0/	
PLOG/3.000E-02	7.55E+22	-3.68	29920.0/	! fit btw. 500 and 2500 K with MAE of 3.6%, 6.4%
PLOG/3.947E-02	1.62E+82	-21.28	56730.0/	
PLOG/3.947E-02	7.48E+22	-3.65	29920.0/	! fit btw. 500 and 2500 K with MAE of 3.4%, 6.7%
PLOG/1.000E+00	4.96E+49	-11.06	44950.0/	
PLOG/1.000E+00	1.10E+70	-15.57	95270.0/	! fit btw. 500 and 2500 K with MAE of 5.3%, 20.1%
PLOG/1.000E+01	5.25E+83	-20.63	68920.0/	
PLOG/1.000E+01	2.69E+26	-4.07	34730.0/	! fit btw. 500 and 2500 K with MAE of 1.5%, 3.7%
PLOG/1.000E+02	4.44E+70	-16.41	67430.0/	
PLOG/1.000E+02	2.06E+23	-2.98	34340.0/	! fit btw. 500 and 2500 K with MAE of 0.7%, 2.1%

C₁₂H₂₅ (5-dodecyl) → C₉H₁₈ (1-nonene) + C₃H₇^b

8.86E+30 -5.14 38830.0

PLOG/3.000E-02	7.43E+33	-6.93	33550.0/	! fit btw. 500 and 2500 K with MAE of 32.6%, 103.5%
PLOG/3.947E-02	2.79E+34	-7.06	34110.0/	! fit btw. 500 and 2500 K with MAE of 31.8%, 96.9%
PLOG/1.000E+00	1.21E+38	-7.68	39060.0/	! fit btw. 500 and 2500 K with MAE of 20.9%, 34.8%
PLOG/1.000E+01	2.52E+36	-6.93	40140.0/	! fit btw. 500 and 2500 K with MAE of 12.2%, 21.1%
PLOG/1.000E+02	8.86E+30	-5.14	38830.0/	! fit btw. 500 and 2500 K with MAE of 9.1%, 24.8%

PLOG/3.000E-02	2.68E+81	-21.17	55480.0/	
PLOG/3.000E-02	1.32E+23	-3.79	30180.0/	! fit btw. 500 and 2500 K with MAE of 3.9%, 7.5%
PLOG/3.947E-02	1.19E+82	-21.31	56230.0/	
PLOG/3.947E-02	1.11E+23	-3.75	30080.0/	! fit btw. 500 and 2500 K with MAE of 3.7%, 6.7%
PLOG/1.000E+00	9.05E+51	-11.78	45810.0/	
PLOG/1.000E+00	1.77E+62	-13.60	84310.0/	! fit btw. 500 and 2500 K with MAE of 5.2%, 20.5%
PLOG/1.000E+01	1.00E+190	-46.61	257700.0/	
PLOG/1.000E+01	1.26E+40	-8.01	42000.0/	! fit btw. 500 and 2500 K with MAE of 6.9%, 23.9%
PLOG/1.000E+02	1.85E+76	-18.08	70290.0/	
PLOG/1.000E+02	2.09E+24	-3.30	34830.0/	! fit btw. 500 and 2500 K with MAE of 0.7%, 2.2%

C₁₂H₂₅ (5-dodecyl) → C₆H₁₂ (1-hexene) + C₆H₁₃^b

1.31E+31 -5.12 38690.0

PLOG/3.000E-02	1.17E+34	-6.91	33450.0/	! fit btw. 500 and 2500 K with MAE of 32.4%, 102.8%
PLOG/3.947E-02	4.37E+34	-7.04	34010.0/	! fit btw. 500 and 2500 K with MAE of 31.7%, 96.2%
PLOG/1.000E+00	1.74E+38	-7.65	38930.0/	! fit btw. 500 and 2500 K with MAE of 20.8%, 34.6%
PLOG/1.000E+01	3.60E+36	-6.90	39990.0/	! fit btw. 500 and 2500 K with MAE of 12.2%, 21.0%
PLOG/1.000E+02	1.31E+31	-5.12	38690.0/	! fit btw. 500 and 2500 K with MAE of 9.1%, 24.8%

PLOG/3.000E-02	3.61E+81	-21.13	55350.0/	
PLOG/3.000E-02	2.14E+23	-3.78	30070.0/	! fit btw. 500 and 2500 K with MAE of 3.9%, 7.5%

PLOG/3.947E-02	1.64E+82	-21.28	56100.0/	
PLOG/3.947E-02	1.80E+23	-3.73	29970.0/	! fit btw. 500 and 2500 K with MAE of 3.6%, 6.8%
PLOG/1.000E+00	1.65E+52	-11.78	45710.0/	
PLOG/1.000E+00	3.42E+56	-12.01	77350.0/	! fit btw. 500 and 2500 K with MAE of 5.1%, 21.0%
PLOG/1.000E+01	4.86E+190	-46.72	258300.0/	
PLOG/1.000E+01	1.69E+40	-7.98	41850.0/	! fit btw. 500 and 2500 K with MAE of 6.9%, 23.9%
PLOG/1.000E+02	2.14E+76	-18.03	70080.0/	
PLOG/1.000E+02	3.14E+24	-3.28	34690.0/	! fit btw. 500 and 2500 K with MAE of 0.7%, 2.2%

C₁₂H₂₅ (6-dodecyl) → C₈H₁₆ (1-octene) + C₄H₉^b

4.39E+31 -5.29 38890.0

PLOG/3.000E-02	3.76E+33	-6.80	33040.0/	! fit btw. 500 and 2500 K with MAE of 33.0%, 107.7%
PLOG/3.947E-02	1.55E+34	-6.94	33620.0/	! fit btw. 500 and 2500 K with MAE of 32.3%, 101.1%
PLOG/1.000E+00	1.50E+38	-7.66	38740.0/	! fit btw. 500 and 2500 K with MAE of 21.7%, 36.0%
PLOG/1.000E+01	6.48E+36	-7.00	40000.0/	! fit btw. 500 and 2500 K with MAE of 12.5%, 22.3%
PLOG/1.000E+02	4.39E+31	-5.29	38890.0/	! fit btw. 500 and 2500 K with MAE of 9.2%, 24.8%

PLOG/3.000E-02	9.65E+80	-21.01	54810.0/	
PLOG/3.000E-02	2.08E+23	-3.80	30170.0/	! fit btw. 500 and 2500 K with MAE of 4.1%, 7.9%
PLOG/3.947E-02	4.00E+81	-21.14	55520.0/	
PLOG/3.947E-02	1.72E+23	-3.75	30030.0/	! fit btw. 500 and 2500 K with MAE of 3.8%, 6.9%
PLOG/1.000E+00	1.40E+53	-12.09	46000.0/	
PLOG/1.000E+00	3.96E+58	-12.61	78870.0/	! fit btw. 500 and 2500 K with MAE of 5.0%, 20.4%
PLOG/1.000E+01	1.29E+41	-8.26	42170.0/	
PLOG/1.000E+01	6.03E+135	-32.35	189200.0/	! fit btw. 500 and 2500 K with MAE of 6.7%, 23.5%
PLOG/1.000E+02	3.29E+76	-18.13	69620.0/	
PLOG/1.000E+02	5.31E+24	-3.36	34740.0/	! fit btw. 500 and 2500 K with MAE of 0.7%, 1.7%

C₁₂H₂₅ (6-dodecyl) → C₇H₁₄ (1-heptene) + C₅H₁₁^b

4.13E+31 -5.29 38860.0

PLOG/3.000E-02	3.62E+33	-6.80	33020.0/	! fit btw. 500 and 2500 K with MAE of 32.9%, 107.5%
PLOG/3.947E-02	1.48E+34	-6.94	33600.0/	! fit btw. 500 and 2500 K with MAE of 32.2%, 100.9%
PLOG/1.000E+00	1.41E+38	-7.65	38720.0/	! fit btw. 500 and 2500 K with MAE of 21.7%, 35.9%
PLOG/1.000E+01	6.09E+36	-6.99	39980.0/	! fit btw. 500 and 2500 K with MAE of 12.5%, 22.3%
PLOG/1.000E+02	4.13E+31	-5.29	38860.0/	! fit btw. 500 and 2500 K with MAE of 9.2%, 24.8%

PLOG/3.000E-02	9.49E+80	-21.01	54800.0/	
PLOG/3.000E-02	1.99E+23	-3.79	30140.0/	! fit btw. 500 and 2500 K with MAE of 4.1%, 7.9%
PLOG/3.947E-02	3.75E+81	-21.13	55500.0/	
PLOG/3.947E-02	1.65E+23	-3.75	30010.0/	! fit btw. 500 and 2500 K with MAE of 3.8%, 6.9%

PLOG/1.000E+00	1.26E+53	-12.08	45970.0/	
PLOG/1.000E+00	4.22E+58	-12.61	78910.0/	! fit btw. 500 and 2500 K with MAE of 5.0%, 20.3%
PLOG/1.000E+01	1.19E+41	-8.25	42140.0/	
PLOG/1.000E+01	8.35E+135	-32.39	189400.0/	! fit btw. 500 and 2500 K with MAE of 6.7%, 23.4%
PLOG/1.000E+02	1.35E+78	-18.59	70740.0/	
PLOG/1.000E+02	7.07E+24	-3.40	34800.0/	! fit btw. 500 and 2500 K with MAE of 0.7%, 2.2%

^aFits have been carried out using the auxiliary MESS_TPfit written by Franklin Goldsmith; see <http://tcg.cse.anl.gov/papr/codes/mess.html>.

^bThe calculations of the rate constant have been performed using a simplified PES including only the direct C-C bond β -scission channel.

References

- (1) Herbinet, O.; Marquaire, P. M.; Battin-Leclerc, F.; Fournet, R., Thermal Decomposition of *n*-Dodecane: Experiments and Kinetic Modeling. *J. Anal. Appl. Pyrolysis* **2007**, *78*, 419-429.
- (2) Dahm, K. D.; Virk, P. S.; Bounaceur, R.; Battin-Leclerc, F.; Marquaire, P. M.; Fournet, R.; Daniau, E.; Bouchez, M., Experimental and Modelling Investigation of the Thermal Decomposition of *n*-Dodecane. *J. Anal. Appl. Pyrolysis* **2004**, *71*, 865-881.
- (3) Malewicki, T.; Brezinsky, K., Experimental and Modeling Study on the Pyrolysis and Oxidation of *n*-Decane and *n*-Dodecane. *Proc. Combust. Inst.* **2013**, *34*, 361-368.
- (4) Banerjee, S.; Tangko, R.; Sheen, D. A.; Wang, H.; Bowman, C. T., An Experimental and Kinetic Modeling Study of *n*-Dodecane Pyrolysis and Oxidation. *Combust. Flame* **2016**, *163*, 12-30.
- (5) Zhou, P. H.; Hollis, O. L.; Crynes, B. L., Thermolysis of Higher Molecular-Weight Straight-Chain Alkanes C9-C22. *Ind. Eng. Chem. Res.* **1987**, *26*, 846-852.
- (6) MacDonald, M. E.; Ren, W.; Zhu, Y.; Davidson, D. F.; Hanson, R. K., Fuel and Ethylene Measurements During *n*-Dodecane, Methylcyclohexane, and *iso*-Cetane Pyrolysis in Shock Tubes. *Fuel* **2013**, *103*, 1060-1068.
- (7) Yu, J.; Eser, S., Thermal Decomposition of C10-C14 Normal Alkanes in Near-Critical and Supercritical Regions: Product Distributions and Reaction Mechanisms. *Ind. Eng. Chem. Res.* **1997**, *36*, 574-584.
- (8) Yu, J.; Eser, S., Kinetics of Supercritical-Phase Thermal Decomposition of C10-C14 Normal Alkanes and Their Mixtures. *Ind. Eng. Chem. Res.* **1997**, *36*, 585-591.